COOPERATIVE TRANSMISSION WITH CONTINUOUS PHASE MODULATION AND PHASE-ONLY FORWARD RELAYS

by

Qi Yang

B.A.Sc(Electronic Engineering), Peking University, 2007

A THESIS SUBMITTED IN PARTIAL FULFILLMENT
OF THE REQUIREMENTS FOR THE DEGREE OF
MASTER OF APPLIED SCIENCE
in the School
of
Engineering Science

SIMON FRASER UNIVERSITY
Spring 2010

APPROVAL

Name: Qi Yang

Degree: Master of Applied Science

Title of Thesis: Cooperative Transmission with Continuous Phase Modulation and Phase-Only Forward Relays

Examining Committee: Dr. Jie Liang, Chair

Chair

Dr. Paul K. M. Ho
Senior Supervisor

Dr. John S. Bird
Supervisor

Dr. Sami Muhaidat
Supervisor

Dr. James K. Cavers
Internal Examiner

Date Approved: April 15, 2010

Declaration of
Partial Copyright Licence

Abstract

We propose in the thesis the concept of Phase-Only Forward (PF) as a possible relay strategy for cooperative communication involving CPFSK and GMSK modulations. The technique enables the relay nodes to maintain constant envelop signaling without the need to perform decoding and signal regeneration. The bit-error-probability (BEP) of this PF scheme in a time-selective Rayleigh fading environment, with noncoherent discriminator detection, was analyzed. Both cases of with and without antenna selection at the relay were considered. In the former case, a clever phase-adjustment scheme that allows the relay to maintain phase continuity at the antenna switching instants was proposed. Results from our BEP analysis show that even without antenna selection at the relay, PF has a lower BEP than conventional decode-and-forward (DF). It also delivers the same performance as amplify-and-forward (AF) when fading is static. In a time selective fading environment, PF is not as efficient as AF when without antenna selection. However with dual-antenna selection at the relay, PF has practically the same performance as AF even in a time-selective fading environment. It can thus be concluded that PF is a cost-effective alternative to AF and DF, since we no longer need signal regeneration nor expensive linear amplifiers at the relays to support non-constant envelop transmission.

Acknowledgments

I am deeply grateful to my supervisor, Dr. Paul Ho for providing a valuable opportunity to work with him, and for training me as a M.Sc. student at Simon Fraser University. Special thanks are due to Dr. John Bird, Dr. Sami Muhaidat and Dr. James Cavers for examining and reviewing this thesis, and to Dr. Jie Liang for chairing my thesis defense.

I would like to thank all members in the RF/Microwave Mobile Communication Laboratory for their support and friendship.

Last but not least, I owe a great deal to my family. I definitely would not be where I am today without their gifts of positivity, understanding, support and everlasting love.

Contents

List of Tables

List of Figures

List of Symbols

Symbol	Definition
$g_i(t)$	Complex channel gain in i-th link
$R(\tau)$	Autocorrelation function
$r_i(t),\ i = 0,1,2$	Received signal in $S-R$, $S-D$, $R-D$ link
G	Amplification factor
$\hat{s}(t)$	Estimated transmit signal
ε	Shadowing factor
$\theta(t)$	Data phase
$\dot{\theta}(t)$	Data phase derivative
$\hat{\theta}(t)$	Estimated data phase
$\hat{\dot{\theta}}(t)$	Estimated data phase derivative
h	Modulation index
b_i	i-th data bit
$\hat{b}_i$	Estimated i-th data bit
T	Bit interval
B	Signal bandwidth
f_D	Maximum Doppler frequency

B_0	3-dB bandwidth of Gaussian pulse
$\psi(t)$	Received signal phase
ψ_R	Forwarded signal phase
$\dot{\psi}(t)$	Received phase derivative
$c(t)$	Before FM modulator GMSK signal
$p(t)$	Rectangular pulse response of a Gaussian low-pass filter
$erf()$	Gauss error function
$y(t)$	Signal fed into discriminator
$u(t)$	Normalized $y(t)$
$z(t)$	Output of discriminator
$a(t)$	Received signal amplitude
γ	Signal variance
σ_n^2	Noise variance
A	Amplification factor
Γ	Adaptive forwarding threshold
D_k	Decision factor
R_i	Complex Gaussian vector
$\varphi(s)$	Characteristic function
s	Transform domain variable
$\|\cdot\|$	Determinant

List of Glossaries

Glossary	Definition
AF	Amplify-and-forward
AWGN	Additive white Gaussian noise
BEP	Bit-error probability
CF	Compress-and-forward
CRC	Cyclic redundancy check
CPFSK	Continuous phase frequency shift keying
CPM	Continuous phase modulation
DBPSK	Differential encoded and detected binary phase shift keying
DF	Decode-and-forward
EGC	Equal gain combining
GMSK	Gaussian Minimum-Shift Keying
GSM	Global System for Mobile Communications
i.i.d	Independent and identically distributed
IVC	Inter-vehicular communication
LPF	Low-pass filter
MIMO	Multiple-input multiple-output

MRC	Maximal ratio combining
MSK	Minimum-Shift Keying
PEP	Pair-wise error probability
PSD	Power spectral density
PSK	Phase Shift Keying
QAM	Quadrature Amplitude Modulation
RF	Radio frequency
SIMO	Single-input multiple-output
SNR	Signal-to-noise ratio
ST	Space-time code

Chapter 1

Introduction

1.1 The Concept of Cooperative Communication

Nowadays, multiple-input multiple-output (MIMO) transmission techniques have attracted much attention in wireless communications, since it offers the benefits of spectrum efficiency and transmit diversity. However, in some conditions it is difficult to use multiple transmit antennas at a wireless agent. For example, a regular cell phone or a wireless sensor usually is not able to carry multiple transmit antennas.

There are a few ways to solve this problem. For example, we can design smaller antennas to fit into the wireless equipment, or use other resources to form a virtual MIMO system. Due to cost and other hardware limitations (for example the size of the antenna array must be several times the wavelength of the RF carrier), the latter method is widely studied in recent years, and a new technique called cooperative transmission is introduced.

Cooperative transmission is a method of creating a virtual MIMO communication channel without resorting to mounting antenna arrays at individual nodes [1]. This idea

can be realized in a multi-user wireless system, since each of the users has its own transmit antenna and with proper cooperation they can "share" with others' transmit antennas. For example, in Fig.1.1 each of the two cellular phones (or wireless terminals in general) has one antenna and cannot individually form a MIMO system. But if we make each of the two cellular phones uses its own antenna to transmit wireless signal to both the base station and other users, and then let the other user processes and forwards the received signal to the base station, we can get two copies of the transmit signals at the base station. Spacial diversity is thus obtained through receiving signals from different locations

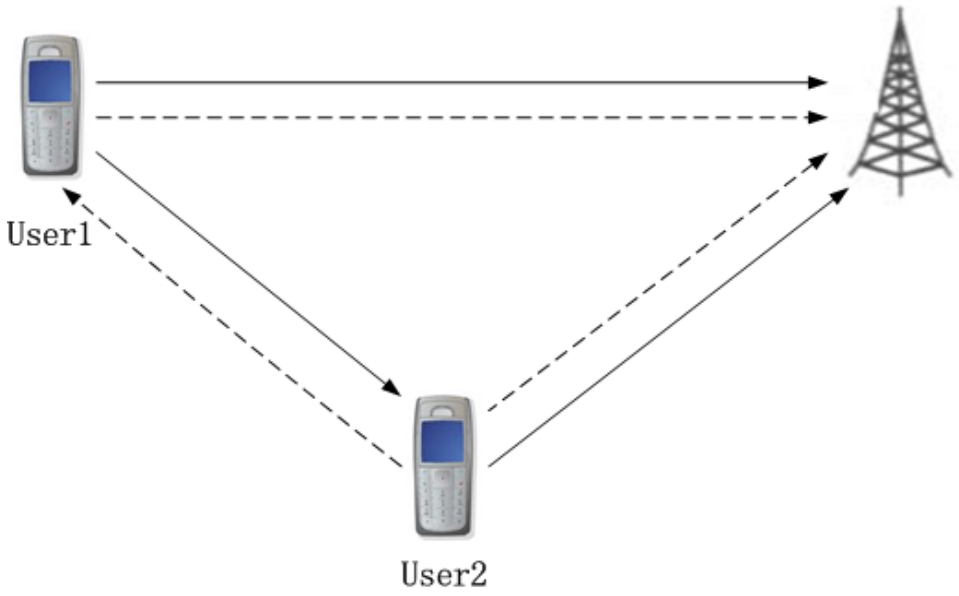

Figure 1.1: Example of a multi-user environment where two mobile terminals form a cooperative communication system.

The aforementioned transmission technique will bring us the benefit of making better use of the multi-user resources. Therefore, cooperative diversity is a cost-effective mean to attain the spatial diversity required to combat fading commonly found in wireless communication systems.

In order to create such a virtual MIMO system researchers proposed a number of relay strategies and companion protocols. In [2], two basic relay strategies for cooperative communication, namely, amplify-and-forward (AF) and decode-and-forward (DF), were considered and their performance evaluated. In AF, the signal received at a cooperating node is simply amplified and relayed to the destination (or other cooperating nodes). No decision will be made at the intermediate nodes. On the other hand in DF, data detection, re-modulation, and retransmission will be performed in that order at the cooperating nodes. Besides DF and AF, in [3] the author mentioned a so-called compress-and-forward (CF) strategy, and in [4] a coded cooperation method is introduced.

Several companion protocols are introduced for cooperative diversity communication. In [5], Nabar, Bölcskei and Kneubuhler proposed three different time-division multiple-access-based cooperative protocols, and analyzed their diversity performance. These protocols involve a single-relay cooperative communication system, and deal with time settings for signal transmission at source, relay and destination. Through the outage probability analysis, a conclusion is obtained that full (second order in this case) spatial diversity can be achieved for some protocols provided that appropriate power control is employed.

MIMO transmission in the form of space-time (ST) code has gained a lot of interest in the wireless community in recent years. Therefore the idea of cooperative transmission in the form of distributed space-time codes naturally emerges. In particular, [5–8] consider the design of a space-time code design for both the AF and DF relays.

Besides analytical result on outage probability, there are also results on symbol error probability. For example, in [9] the exact symbol error probability of a cooperative

network adopting a distributed single-input-multiple output (SIMO) protocol and maximal ratio combining (MRC) was derived for the Rayleigh fading channel. A pair-wise error probability (PEP) analysis of the same protocol was performed in [10] for the log-normal fading case.

1.2 Antenna Selection in Cooperative Communication

In wireless communications, multichannel reception is a classical and effective technique to combat deep signal fades in a Rayleigh-fading channel [11]. When a signal is sent, the receiver will get multiple replicas through different fading channels, and it will combine or select these replicas by using certain rules. There are a few combining schemes, for example the mentioned MRC scheme and the equal gain combining (EGC) scheme. On the other hand, selecting scheme is also widely used as it performs diversity with the least system complexity. [11–14] provide some research results on both combining and selection.

With cooperative relaying techniques developing, a number of strategies for relay selection and antenna selection have been proposed. For example in [15, 16] multiple relays selection was considered, and in [17–19] multi-antenna selection in cooperative communication was studied. The common goal of these antenna selection schemes is to improve the quality of the source-relay link(s), so that the underlying cooperative communication system can deliver the promised performance.

1.3 Motivations and Contributions of the Thesis

Most of the work on cooperative communication, including those mentioned above, share a number of common features: linear modulations such as Phase Shift Keying (PSK) and Quadrature Amplitude Modulation (QAM), block fading, coherent detection, and conventional AF and/or DF relay modes. Departures from these standard configurations are rare. In [20], the authors do consider differential detection of distributed differential ST block codes. However, fading is still assumed to be block-wise static and the modulation is again linear. In [21], Maw et. al. part with linear modulation and consider a relay system that employs constant envelop continuous phase frequency shift keying (CFPSK), distributed ST trellis codes, and a novel multiple relay protocol. From the transmission point of view, CPFSK and in general continuous phase modulation (CPM) [22], has an advantage over linear modulation because they enable the use of inexpensive non-linear (e.g. Class C) power amplifiers. As a matter of fact, the well-known GSM cellular standard and many private mobile radio networks employ this type of modulations. However, the use of constant envelop modulation in [21] is restricted to the source terminal, as the relays still adopt AF. In our opinion, the use of AF at the relays actually contradicts the rationale of using constant envelop signaling in the first place. Furthermore, the work in [21] is confined to static fading and coherent detection.

In this thesis, we consider a single-relay cooperative communication system that employs constant envelop signal with time-selective fading. This SIMO system adopts Protocol II in [5], with two common-used modulation schemes - CPFSK (including MSK) and Gaussian Minimum-Shift Keying (GMSK), and discriminator detection is applied. A

potential application of this scheme is inter-vehicular communication (IVC) where vehicles in proximity of the sending node will relay the information to the destination node. Because of the mobility of the participating nodes, "fast" or time-selective fading is inevitable, making coherent detection challenging. This is the rationale behind adopting non-coherent discriminator detection.

Furthermore, since data information is only embedded in the phase of the constant envelop signal, we explore the idea of phase-only forward (PF) at the relaying node as a mean to maintain constant envelop transmission throughout the signaling chain. This new forwarding scheme ensures that the signal amplitude sent at the relay is constant, and therefore allows the use of inexpensive Class C power amplifiers at the relay. PF is thus more cost effective than AF. Moreover, when compared to decode-and-forward, PF has less processing complexity at the relay because it does not require detection and recoding. It will lead to less delay and a smaller cost than DF (In this thesis the decode-and-forward scheme is actually detect-and-forward scheme). To analyze the performance of phase-only-forward, we derive semi-analytical expressions for the bit-error probability (BEP) of both CPFSK and GMSK, followed by simulations for both static and fast fading channels. Through the analysis and simulation, we find that without antenna selection, PF performs better than DF in a static fading channel, and more or less the same as AF. In a time-selective or "fast" fading channel though, PF is worse than AF. However, the reader is reminded that once the system designer chooses constant envelop as the modulation scheme, then he/she implicitly rules out AF at the same time because this relaying strategy is inconsistent with the rational of using this type of modulations in the first place. The results on AF in this case will thus serve nothing more than an indicator of what could be

obtained if we relax the constant envelop constraint at the relay.

To further improve the PF scheme, we consider dual antenna selection at the relay. Since the two signals received at the relay usually don't have the same phase, we invent a clever phase adjustment scheme to maintain phase continuity when switching between the two antennas. This allows the PF relay to transmit a continuous-phase constant envelop signal, just like the original data signal transmitted by the source. Also, semi-analytical expressions for the bit-error probability (BEP) of PF with dual antenna selection are derived, and simulation results are used to prove their correctness. From the results we can see the performance of PF with dual antenna selection at relay is better than AF without antenna selection for both static fading channel and fast fading channel.

The last contribution of the thesis is to make a performance comparison between cooperative transmission and time diversity in a fast fading channel. We show the simulation results for PF with dual antenna selection and time diversity from both bit-error probability and outage probability point of view. We found that PF with dual antenna selection still performs more reliable than time diversity.

1.4 Thesis Outline

The Thesis is organized as follows. We first present in Chapter 2 the transmission and fading models adopted in this investigation. Then the corresponding discriminator detector and the proposed phase-only-forward method involving CPFSK modulation are introduced in Chapter 3, along with the derivation of semi-analytical expressions of the BEP performance. To confirm the accuracy of these expressions we also provide simulation

results in this chapter. In Chapter 4 we make two extensions of the new PF scheme: PF with GMSK modulation and PF with antenna selection. A clever phase adjustment scheme is introduced to support phase continuity during antenna selection. Similar to Chapter 3, both analytical and simulation result are provided. Finally, we summarize the major findings of this investigation and suggest topics for future research in Chapter 5.

Chapter 2

Signal and System Model

In this chapter, we provide details of elements of the cooperative communication systems considered in this thesis. Section 2.1 describes both the basic cooperative communication and the channel model. Then properties of the modulation schemes used in the our cooperative communication system, namely continuous phase modulations (CPM), are described in Section 2.2. Section 2.3 focuses on the demodulation aspect. Specifically, the optimal symbol-by-symbol non-coherent detector of CPM is re-derived.

2.1 Cooperative Transmission and Fading Models

Our cooperative transmission system is a single-relay system. This system comprises of three nodes, a sending node S, a single relay node R, and a destination node D, and it adopts the so-called Protocol II in [5] as the cooperative transmission protocol; refer to Fig. 2.1. With this protocol, S and R transmit their signals in alternate time slots, where each slot comprises of multiple data bits. In the first time slot of each cycle, S sends a signal to

both R and D, which are both in the listening mode. In the second time slot, S enters the silent mode while R relays the signal it received earlier from S to D. The destination D then combines the signals it receives in the two slots and performs data detection. It should be clear that this model can be easily extended to multiple relay nodes, resulting in a virtual SIMO communication system.

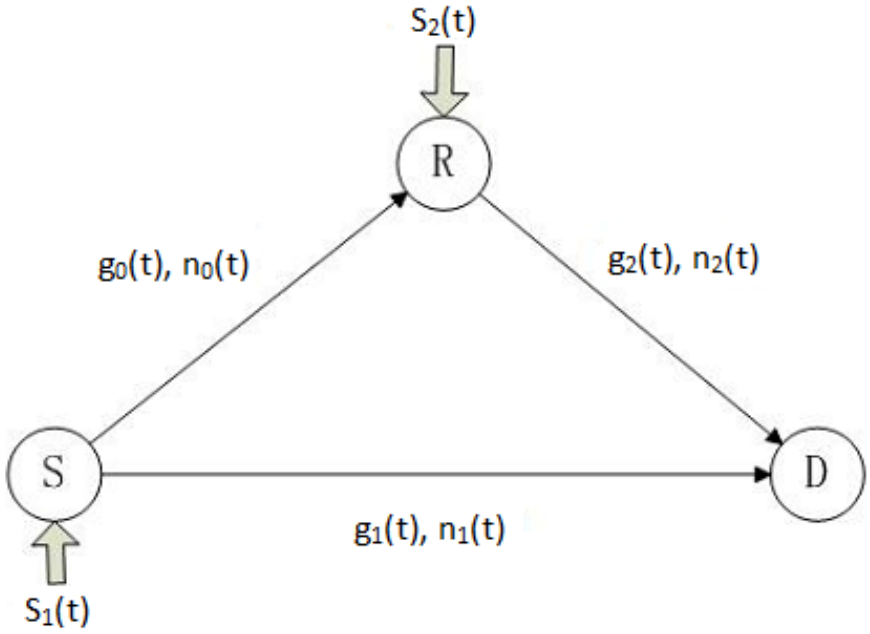

Figure 2.1: Cooperative communication model.

We assume the signals transmitted through the $S-R$, $S-D$, and $R-D$ links in Fig. 2.1, all experience Rayleigh flat fading and additive Gaussian noise. Using a complex baseband model [14], fading in the three links are represented by the independent, zero-mean complex Gaussian processes $g_0(t)$, $g_1(t)$ and $g_2(t)$, respectively. Assuming isotropic scattering, then each $g_i(t)$ has a Jakes power spectral density (PSD) function, or equivalently the autocorrelation functions:

$$R_{g_i}(\tau) = \frac{1}{2}E\left[g_i^*(t)g_i(t+\tau)\right] = \gamma_i J_0(2\pi f_i \tau); \qquad i = 1,2,3, \tag{2.1}$$

where γ_i is the variance, f_i is the Doppler frequency, and $J_0(\cdot)$ is the zero-th order Bessel function. In addition to fading, each of the $S-R$, $R-D$ and $S-D$ links in Fig. 2.1 introduces additive white Gaussian noise (AWGN). We denote these complex Gaussian processes as $n_0(t)$, $n_1(t)$ and $n_2(t)$ respectively. These processes are statistically independent and identically distributed (i.i.d), each being a zero-mean, complex, band-limited white Gaussian process with power-spectral density N_0 and two-sided bandwidth B. Consequently, their autocorrelation functions are

$$R_{n_i}(\tau) = \tfrac{1}{2}E\left[n_i^*(t)n_i(t+\tau)\right] = N_0 B\,\mathrm{sinc}(B\tau), \tag{2.2}$$

where $\sigma_n^2 = N_0 B$ is the noise power. Without loss of generality, the noise bandwidth is chosen to equal the bandwidth of the transmitted signal described next.

Let $s_1(t)$ and $s_2(t)$ be the unit-energy signals transmitted by the source and the relay in Fig. 2.1. The corresponding signals received in the $S-R$, $S-D$, and $R-D$ links are respectively

$$r_0(t) = g_0(t)s_1(t) + n_0(t), \tag{2.3}$$

$$r_1(t) = g_1(t)s_1(t) + n_1(t), \tag{2.4}$$

$$r_2(t) = g_2(t)s_2(t) + n_2(t), \tag{2.5}$$

With amplifiy-and-forward (AF), the signal $s_2(t)$ assumes the form

$$s_2(t) = G \cdot r_0(t), \tag{2.6}$$

where G is the amplification factor that satisfies the unit-energy constraint. On the other hand with decode and forward (DF), the received signal at the relay will first be demodulated and the data decisions will be used to regenerate the signal

$$s_2(t) = \hat{s}_1(t). \tag{2.7}$$

With an ideal $S-R$ link, $s_2(t) = s_1(t)$. In both cases, the relayed signal $s_2(t)$ is directly related to the information signal $s_1(t)$, so the destination receiver has actually two copies of the same signal, resulting in a potential second order diversity effect.

In this thesis, we will introduce a new relaying technique called phase-only forward (PF) to be used with a class of constant envelop modulations called continuous-phase modulated (CPM). Fig. 2.2 shows the system block diagram of our cooperative communication system with CPM modulation and non-coherent discriminator detection. Details of the operations performed by the PF relay will be described in the next chapter of the thesis, whereas properties of CPM and the rationale for using these modulations in cooperative communication are presented in the next section.

Finally, we point out that while the focus of this investigation is Rayleigh fading, we will also provide some results in a later chapter on the effect of shadowing in the above cooperative communication system. In wireless communication, when the mobile terminal moves through a terrain, it often enters "shadows" created by obstacles, for examples a tall building or a small hill. These natural or man-made objects will attenuate the received signal level at the destination. This is called shadowing effect and a common statistically model that describes its behavior is the log-normal distribution [23]. In this thesis we model the shadowing fading effect as following:

$$r_0(t) = g_0(t)s_1(t) + n_0(t), \tag{2.8}$$

$$r_1(t) = \varepsilon g_1(t)s_1(t) + n_1(t), \tag{2.9}$$

$$r_2(t) = \varepsilon g_2(t)s_2(t) + n_2(t), \tag{2.10}$$

where ε is the shadowing factor in the log-normal distribution. As shown in (2.8), (2.9) and (2.10) we consider shadowing effect only in the $S-D$ and $R-D$ links. A variance of 8dB in the long-term fading is considered.

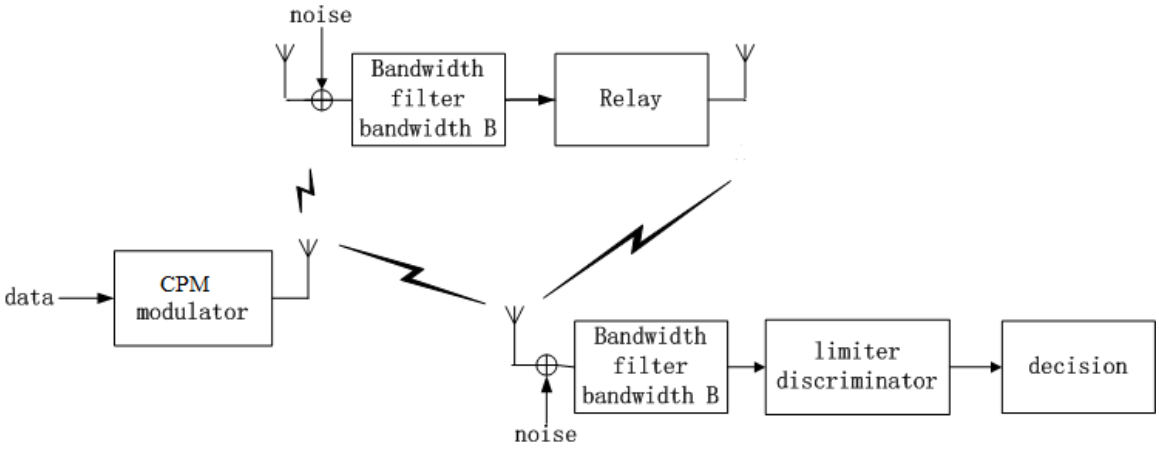

Figure 2.2: Block diagram of a CPFSK cooperative communication system.

2.2 Continuous Phase Modulation

In wireless communications, continuous phase modulation (CPM) is a widely used modulation scheme. For example in GSM, one of the world's 2nd generation cell phone systems, a CPM scheme called Gaussian minimum shift keying (GMSK) modulation is used. CPM has also been used in Bluetooth, 802.11 FHSS etc. Compared to some

other phase modulation schemes, CPM's carrier phase is modulated continuously and that can lead to good power spectrum efficiency. Furthermore, CPM is a constant envelop modulation scheme. The data information is only embedded in the CPM signal's phase. So if we choose CPM as the modulation scheme in our cooperative communication system, we can use inexpensive non-linear amplifiers such as Class C amplifiers.

In general, a CPM signal assumes the form

$$s(t) = \exp\{j\theta(t)\},, \tag{2.11}$$

where $\theta(t)$ is the data dependent phase. Although different ways of generating $\theta(t)$ from the data give us different CPM schemes, they all share the common features of constant envelop and continuous phase. In the following, we focus on two specific CPM schemes: continuous-phase frequency-shift-keying (CPFSK) and Gaussian Minimum-Shift-Keying (GMSK).

2.2.1 Continuous-Phase Frequency-Shift Keying

In CPFSK, the data-dependent phase changes linearly within a symbol interval. Specifically,

$$\theta(t) = \pi h \left(\sum_{i=0}^{k-1} b_i \right) + \pi h b_k (t - kT)/T, \qquad kT < t \leq (k+1)T, \tag{2.12}$$

where $b_k \in \{\pm 1\}$ is the k-th data bit, $0 < h < 1$ is the modulation index, T is the bit interval, and $1/T$ is the bit rate. As shown in [22], increasing the modulation index usually leads to an improvement in data reliability, at the expense of bandwidth expansion. Fig. 2.3, 2.4, and 2.5 show the power spectrum of CPFSK with different modulation indices: h=1/4, 1/2,

and 3/4.

As observed from these figures, the power spectrum of CPFSK is, strictly speaking, not bandlimited. In this investigation, we adopt both the 99% and 99.9% bandwidth definition in [22]. Using (4.4.51)-(4.4.52) of [14], we obtain the bandwidth of the binary CPFSK schemes listed in Table 2.1. Subsequently, the bandwidth B in (2.2) is set to the corresponding values in the table when these schemes are considered. Note that the case of $h = 1/2$ corresponds to the well known Minimum Shift Keying (MSK) scheme [22].

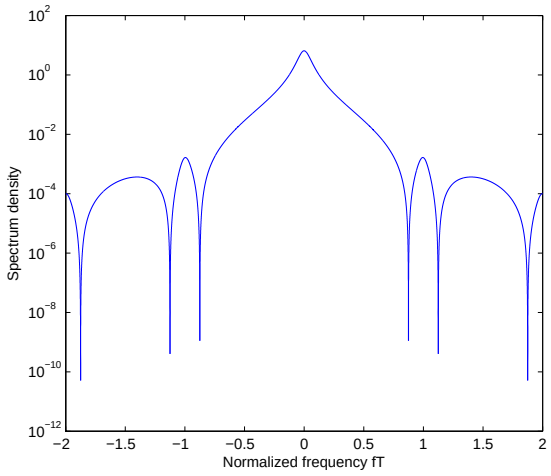

Figure 2.3: Spectrum density for CPFSK signal with h=1/4

Modulation Index h	1/4	1/2	3/4
99% Bandwidth BT	0.8980	1.1818	1.8562
99.9% Bandwidth BT	1.4202	2.7330	3.6480

Table 2.1: Normalized bandwidth of binary CPFSK schemes.

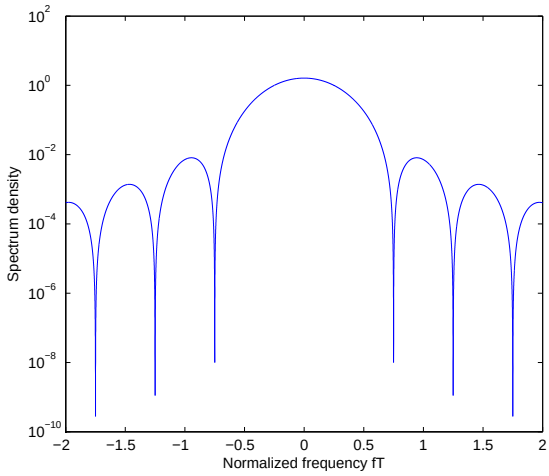

Figure 2.4: Spectrum density for CPFSK signal with h=1/2

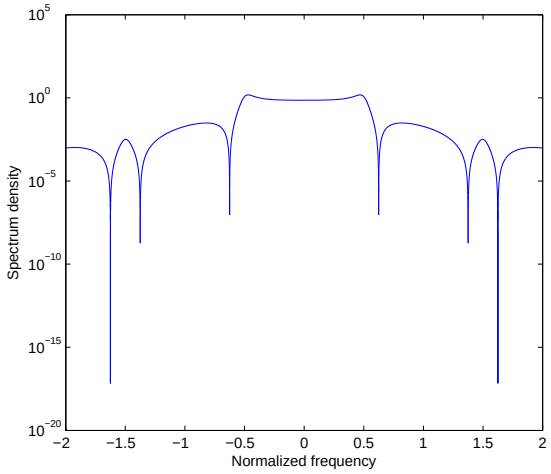

Figure 2.5: Spectrum density for CPFSK signal with h=3/4

2.2.2 Gaussian Minimum-Shift Keying

From (2.12), one can deduce that CPFSK uses a rectangular frequency pulse. Because of the discontinuities at the two ends of this pulse, the PSD of CPFSK decays with frequency at a rate of $|f|^{-4}$. To achieve a more compact spectral characteristic, a smoother frequency pulse should be used. One good example is the so-called Gaussian MSK [14] (or GMSK). In an GMSK system, like the one shown in Fig. 2.6, the modulator at the source S first generates the baseband signal.

$$c(t) = \sum_{n=-\infty}^{\infty} b_n p(t - nT), \tag{2.13}$$

where the b_n 's are the random binary data with ± 1 values and

$$p(t) = \frac{A}{2}\left[erf\left(-\sqrt{\frac{2}{\ln 2}}\pi B_0\left(t-\frac{T}{2}\right)\right) + erf\left(\sqrt{\frac{2}{\ln 2}}\pi B_0\left(t+\frac{T}{2}\right)\right)\right], \qquad t > 0 \tag{2.14}$$

is the rectangular pulse response of a Gaussian low-pass filter. Then $c(t)$ will be fed into a FM modulator to generate the GMSK signal.

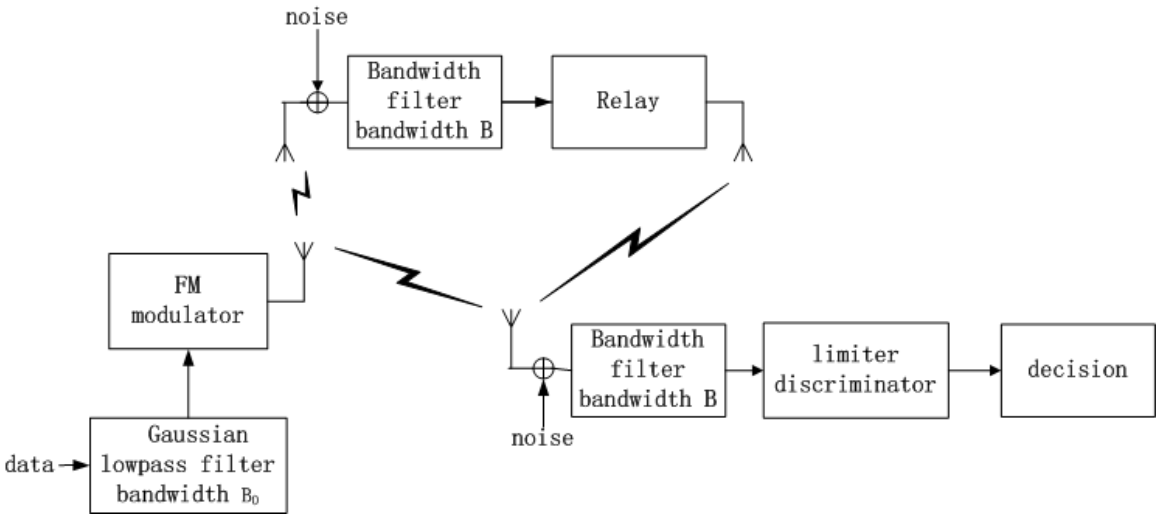

Figure 2.6: Block diagram of GMSK cooperative communication system.

In (2.14) the parameter B_0 is the 3-dB bandwidth of the Gaussian pluse. Strictly speaking, this pulse is not time-limited. In practical applications, the pulse is usually truncated to some specified fixed duration. GMSK with $B_0T = 0.3$ is used in the European digital cellular communication system called GSM [14]. In this thesis we adopt the so-called GMSK-6 scheme in [24] and set the Gaussian LPF 3dB bandwidth to $B_0T = 0.3$. Its spectrum density is shown in Fig. 2.7.

After feeding (2.14) to an FM modulator, the source S generates the CPM signal

$$s(t) = \exp\left(j\int_{-\infty}^{t} c(\tau)d\tau\right) = \exp\left(j\theta(t)\right), \tag{2.15}$$

where $\theta(t)$ is the information-bearing phase. This signal has a 99% bandwidth [22] of $BT = 0.91$ [24]. Fig. 2.8 shows the power density spectrum of the GMSK signal with $B_0T = 0.3$.

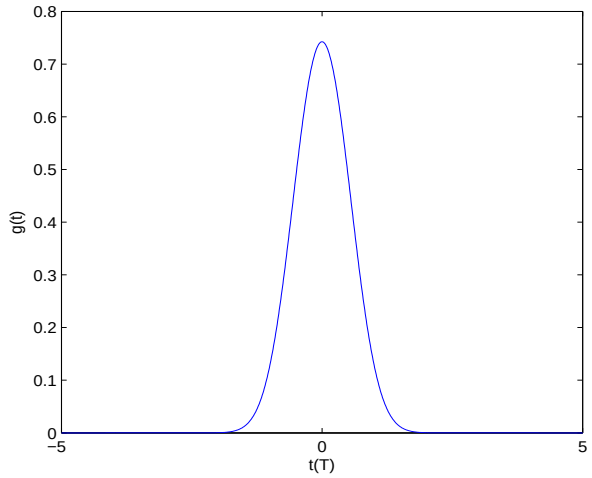

draft

Figure 2.7: Pulse shape of GMSK signal with $B_0T = 0.3$

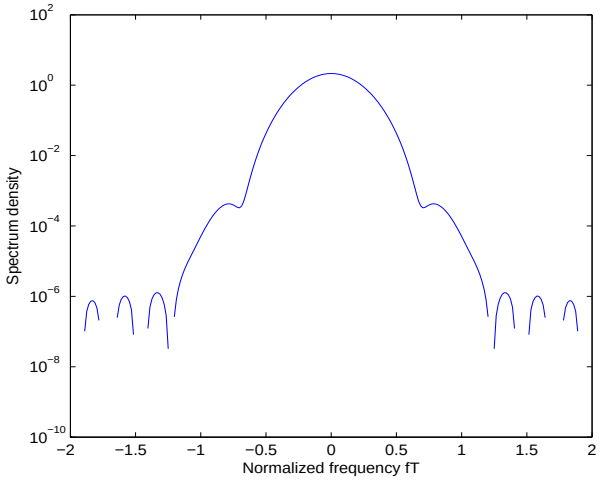

Figure 2.8: Spectrum density for GMSK signal with $B_0T = 0.3$

2.3 Demodulation of CPM

The received signals at the destination (and at the relay, in the case of DF) can be detected coherently or non-coherently. Coherent detection requires channel tracking and usually comes in the form of a Viterbi decoder [14]. Both components require substantial computations and decoding delay, not to mention the need to transmit pilot symbols for channel sounding purpose. On the other hand, non-coherent detection does not require any channel estimation and it allows symbol-by-symbol detection. From an implementation point of view, it is much simpler, though its error performance is not as good as coherent detection. In this investigation, we focus on non-coherent discriminator detection [25]. This detector examines the phase derivative of the received signal and from its polarity, determine whether the data bit b_k is a $+1$ or a -1.

2.3.1 Discriminator Detector Model

The received CPM signal will first pass through a low-pass filter to limit the amount of noise. Then it will be feed into the discriminator. Fig. 2.9 shows the baseband receiver model. Assuming the signal after noise limiting in Fig. 2.2 is

$$r(t) = a(t)\exp(j\psi(t)), \tag{2.16}$$

where $a(t)$ is the amplitude and $\psi(t)$ is the phase. The objective of discriminator detection is to generate the phase derivative and this is done as follows. We first normalize $r(t)$ to the constant envelop signal

$$u(t) = \frac{r(t)}{|r(t)|} = \exp[j\psi(t)]. \tag{2.17}$$

Then after taking the derivative of $u(t)$ and multiplying it with $-j$ its own conjugate, we obtain

$$z(t) = \dot{u}(t)\cdot[-ju(t)^*] = \dot{\psi}(t), \tag{2.18}$$

which is actually the phase derivative $\dot{\psi}(t)$. As we described before, the data information of CPM signal is only embedded in the phase derivative $\dot{\theta}(t)$, and $\dot{\psi}(t)$ is a noise version of $\dot{\theta}(t)$, so we can use $z(t)$ to make data decision. Considering we sample the receiver output $z(t)$ at $t = nT$, if $z(nT)$ is positive, the decision on the data bit is a $+1$, else the decision will be a -1.

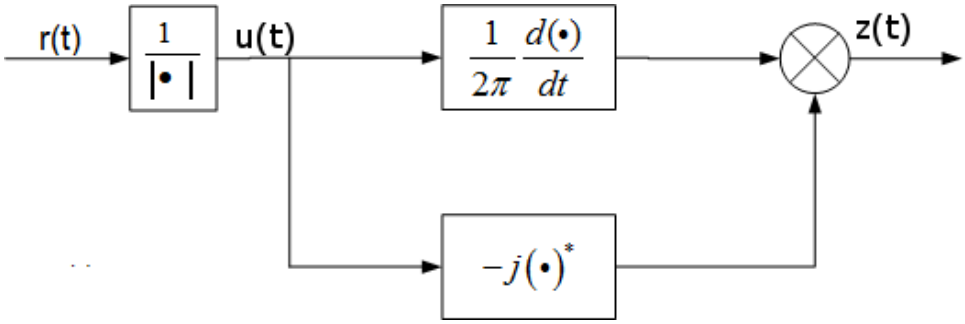

Figure 2.9: Model of the Discriminator

2.3.2 Statistic of Discriminator Detector

Consider continuous phase modulation (CPM) and Rayleigh flat fading. In this case the received signal in (2.16) takes on the form

$$r(t) = g(t)e^{j\theta(t)} + n(t) = a(t)e^{j\psi(t)}, \tag{2.19}$$

where $\theta(t)$ is the data-dependent phase of the CPM signal, $g(t)$ and $n(t)$ are zero-mean complex Gaussian processes with variances γ and σ_n^2 respectively, and $a(t)$ and $\psi(t)$ are respectively the amplitude and phase of $r(t)$. The autocorrelation functions of $g(t)$ and $n(t)$ are respectively $\gamma J_0(2\pi f_D \tau)$ and $N_0 B\text{sinc}(\text{B}\tau)$; refer to (2.1) and (2.2). The derivatives of $\theta(t)$, $a(t)$ and $\psi(t)$ are denoted as $\dot{\theta}(t)$, $\dot{a}(t)$ and $\dot{\psi}(t)$ respectively. According to (2.12), for CPFSK modulation, $\dot{\theta}(t) = \pi h b_k/T$ in the k-th bit interval. For notation brevity, and also because of the symbol-by-symbol nature of the detection process, we take the liberty of dropping the time variable when describing these random processes from hereon. As shown in [25], given the data phase derivative $\dot{\theta}$, the joint probability density function

(pdf) of $a, \dot{a}, \psi, \dot{\psi}$ at any instant within the k-th symbol interval is

$$p(a,\dot{a},\psi,\dot{\psi}|\dot{\theta}) = \frac{a^2}{4\pi^2\alpha^2\beta^2(1-\rho^2)} \exp\left\{-\frac{\dot{a}^2}{2\beta^2(1-\rho^2)}\right\} \times \exp\left\{-\frac{a^2}{2\beta^2(1-\rho^2)}\left[\left(\dot{\psi}-\rho\frac{\beta}{\alpha}\right)^2 + \frac{\beta^2}{\alpha^2}\left(1-\rho^2\right)\right]\right\}, \tag{2.20}$$

where

$$\begin{aligned}
\alpha^2 &= \tfrac{1}{2}E\left[|r(t)|^2\right] = \gamma + \sigma_n^2, \\
\beta^2 &= \tfrac{1}{2}E\left[|\dot{r}(t)|^2\right] = \gamma\dot{\theta}^2 + \lambda + \sigma_{\dot{n}}^2, \\
\lambda &= \tfrac{1}{2}E\left[|\dot{g}(t)|^2\right] = 2\pi^2 f_D^2\gamma, \\
\sigma_{\dot{n}}^2 &= \tfrac{1}{2}E\left[|\dot{n}(t)|^2\right] = \pi^2 B^2\sigma_n^2/3, \\
\chi^2 &= j\tfrac{1}{2}E\left[r(t)\dot{r}^*(t)\right] = \gamma\dot{\theta}, \\
\rho &= \chi^2/(\alpha\beta) = \gamma\dot{\theta}/(\alpha\beta).
\end{aligned} \tag{2.21}$$

From this pdf we can also obtain some useful marginal pdfs, for example

$$p(a,\dot{a},\dot{\psi}|\dot{\theta}) = \frac{a^2}{2\pi\alpha^2\beta^2(1-\rho^2)} \exp\left[\frac{-\dot{a}^2}{2\beta^2(1-\rho^2)}\right] \times \exp\left\{\frac{-a^2}{2\beta^2(1-\rho^2)}\left[\left(\dot{\psi}-\rho\frac{\beta}{\alpha}\right)^2 + \frac{\beta^2}{\alpha^2}(1-\rho^2)\right]\right\}, \tag{2.22}$$

$$p(a,\dot{\psi}|\dot{\theta}) = \frac{a^2}{\alpha^2\sqrt{2\pi\beta^2(1-\rho^2)}} \exp\left\{\frac{-a^2}{2\beta^2(1-\rho^2)}\left[\left(\dot{\psi}-\rho\frac{\beta}{\alpha}\right)^2 + \frac{\beta^2}{\alpha^2}(1-\rho^2)\right]\right\}, \tag{2.23}$$

and

$$p(\dot{\psi}|\dot{\theta}) = \frac{\beta^2(1-\rho^2)}{2\alpha^2}\left[\left(\dot{\psi}-\rho\frac{\beta}{\alpha}\right)^2 + \frac{\beta^2}{\alpha^2}(1-\rho^2)\right]^{-\frac{3}{2}}. \tag{2.24}$$

The last equation relates the received phase derivative to the data phase derivative. The severity of fading and noise will determine how broad this probability density function is. Specifically, we can derive from these pdfs the bit-error probability (BEP) of Continuous Phase Modulation with discriminator detection and no cooperation. As an example, consider the case of CPFSK. If the data bit is $+1$, the signal phase derivative sent by the

source will be $\dot{\theta} = \frac{\pi h}{T}$. At the receiver, the decision threshold is set at zero. A wrong decision will be made when the received signal phase derivative $\dot{\psi}$ is less than zero. This probability can be expressed as

$$\Pr\left[\dot{\psi} < 0 | \dot{\theta} = \frac{\pi h}{T}\right] = \int_{-\infty}^{0} \int_{0}^{2\pi} \int_{-\infty}^{\infty} \int_{0}^{\infty} p\left(a, \dot{a}, \psi, \dot{\psi} | \dot{\theta} = \frac{\pi h}{T}\right) da d\dot{a} d\psi d\dot{\psi}, \tag{2.25}$$

or equivalently

$$Pr\left[\dot{\psi} < 0 | \dot{\theta} = \frac{\pi h}{T}\right] = \int_{-\infty}^{0} p\left(\dot{\psi} | \dot{\theta} = \frac{\pi h}{T}\right) d\dot{\psi}, \tag{2.26}$$

which after simplification gives us

$$\Pr\left[\dot{\psi} < 0 | \dot{\theta} = \frac{\pi h}{T}\right] = \frac{1}{2}\left(\frac{\gamma^2 \dot{\theta}}{\alpha^2 \beta^2}\right). \tag{2.27}$$

The last equation is the BEP of binary CPFSK in a Rayleigh fading channel with limiter discriminator detection. In this thesis, it also represents the BEP at the relay of a decoded-and-forward cooperative network that employs CPFSK.

Chapter 3

Cooperation with CPFSK and Phase-Forward Relays

In this chapter we consider a single relay cooperative communication system that employs CPFSK modulation with time-selective fading. In Section 3.1 we first introduce the two basic forwarding strategies: conventional decode-and-forward (DF) and amplify-and-forward (AF), and then propose a new forwarding strategy called phase-forward (PF). In Section 3.2 we analyze the performance of phase-forward as well as decode-and-forward. Finally Section 3.3 shows the simulation result of the proposed system.

3.1 Phase-Forward Relays

3.1.1 Conventional Decode-and-Forward and Amplify-and-Forward

In Section 2.1 we discuss our cooperative communication model in a general way. Now let's focus on the operation of the relay.

As we show in Fig. 2.1, the relay first receives the signal sent by the source and then forwards it to the destination. The transmitted signal experiences fading and noise and therefore the information forwarded to the destination by the relay could become unreliable. If a severely corrupted signal is forwarded, the performance may be even worse than no cooperation. In [2] the author proposed two basic relaying strategies called decode-and-forward (DF) and amplify-and-forward (AF). In DF, the relay will first detect the signal and make data decision, and then use the data to regenerate the signal and send it to the destination. In our system, this procedure can be represented by

$$\hat{s}(t) = \exp\left\{ j\hat{\theta}(t) \right\}, \tag{3.1}$$

where $\hat{s}(t)$ is the forwarded CPFSK signal and

$$\hat{\theta}(t) = \pi h \left(\sum_{i=0}^{k-1} \hat{b}_i \right) + \pi h \hat{b}_k (t - kT)/T, \qquad kT < t \leq (k+1)T, \tag{3.2}$$

where $\hat{b}_k \in \{\pm 1\}$ is the estimated k-th data bit. On the other hand, in AF, the relay is not asked to detect the signal but only amplifies the CPFSK signal it received. In this case, the forwarded signal becomes

$$\hat{s}(t) = r_0(t)/\sqrt{\gamma + \sigma_n^2}, \tag{3.3}$$

where $r_0(t)$ is the received signal at the relay, and $1/2E\left[|r_0(t)|^2\right] = \gamma + \sigma_n^2$. It should be pointed out that the amplification factor $A = 1/\sqrt{\gamma + \sigma_n^2}$ in (3.3) ensures the signal has the same unit average power as the DF signals in (3.1). When fading is static, cooperative transmission benefits most from adaptive relaying. For example, one can construct an adaptive DF system by passing the decisions $\{\hat{b}_k\}$ obtained from $r_0(t)$ defined in (2.3) to a cyclic redundancy check (CRC) [26]. If the decisions are deemed reliable, the relay then regenerates and forwards the CPFSK signal to the destination. On the other hand, if

the decisions fail the CRC, the relay will refrain from transmission in the second phase. Similarly, an adaptive AF system will only forward the signal to the destination if $|g_0(t)|$ in (2.3) (or other statistics like SNR, likelihood ratio, etc.) is greater than a certain threshold Γ [27]. While both the CRC and the SNR threshold are proper indicators of the $S-R$ link's signal quality, their effectiveness is restricted to the block fading scenario. In fast fading applications like IVC, the transmission in any link will go through multiple fade-cycles, making the CRC fails consistently, and the probability of finding a time instant which $|g(t)| < \Gamma$ approaches unity. In other word, the relay will never transmit if it adopts these reliability tests in a fast fading environment, rendering cooperation meaningless. In this investigation, we will thus consider only fixed forward, i.e., the relay will always transmit a replica of the original signal to the destination.

3.1.2 Phase-Forward

In this thesis, we propose a new relaying strategy called phase-forward. The main idea of phase-forward is to let the relay forward the signal phase it received to the destination. The transmitted signal is the CPFSK signal $s(t) = \exp\{j\theta(t)\}$ in (2.11). The received signals at the relay and at the destination in the first time slot are respectively $r_0(t)$ and $r_1(t)$, where

$$r_i(t) = g_i(t)\exp\{j\theta(t)\} + n_i(t), \qquad i = 0, 1, \tag{3.4}$$

because of the flat fading, $g_i(t)$, and additive noise, $n_i(t)$, mentioned earlier. In polar form, these signals can be rewritten as

$$r_i(t) = a_i(t)\exp\{j\psi_i(t)\}, \qquad i = 0, 1, \tag{3.5}$$

where $a_i(t) = |r_i(t)|$ is the magnitude and $\psi_i(t) = \arg(r_i(t))$ is the phase. In the proposed phase-only forward (PF) scheme, the relay node simply forwards the signal

$$\hat{s}(t) = \exp\{j\psi_R(t)\}, \qquad \psi_R(t) = \psi_0(t), \tag{3.6}$$

where ψ_0 is the received signal phase at the relay shown in Fig. 3.1 and ψ_R is our general notation for the forwarded signal phase. No intermediate decisions will be made. Inevitably, $\psi_0(t)$ will contain phase noise. However, as long as the signal-to-noise ratio (SNR) in the $S-R$ link is sufficiently large, $\psi_0(t)$ should closely resemble the data phase $\theta(t)$ and the forwarded signal (in conjunction with $r_1(t)$) can thus help in producing a diversity effect at the destination.

As in the case of DF and AF, PF is considered to be fixed without adaptive forwarding.

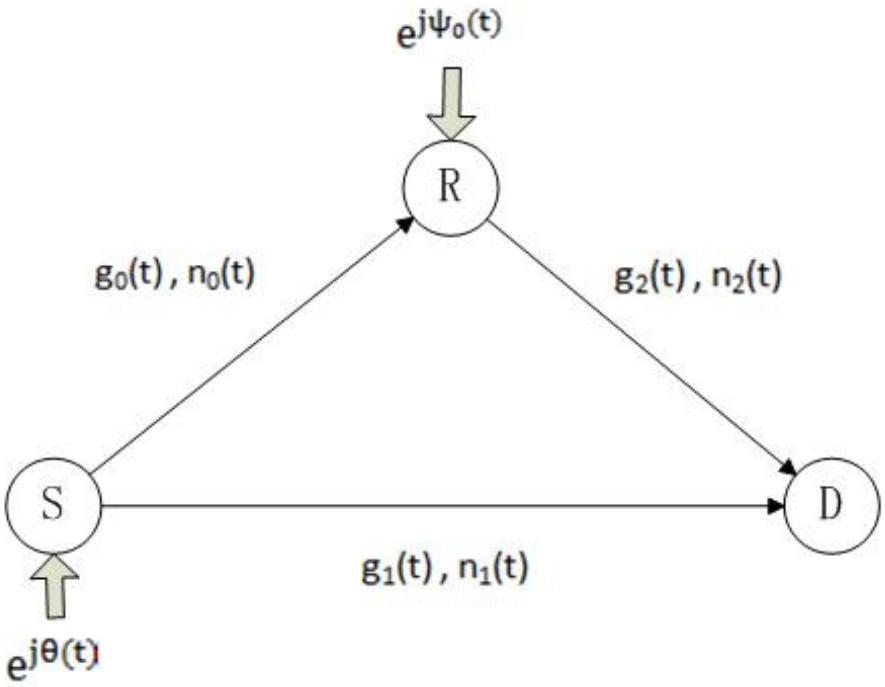

Figure 3.1: Cooperative communication model that employs CPFSK modulation.

3.1.3 Decision Rule with Cooperative Transmission

With cooperative transmission and PF relays, the destination has two corrupted copies of the same phase information:

$$r_1(t) = g_1(t)e^{j\theta(t)} + n_1(t) = a_1(t)e^{j\psi_1(t)}, \tag{3.7}$$

and

$$r_2(t) = g_2(t)e^{j\psi_R(t)} + n_2(t) = a_2(t)e^{j\psi_2(t)}, \tag{3.8}$$

where $a_1(t)$ and $a_2(t)$ are the amplitudes, and $\psi_1(t)$ and $\psi_2(t)$ are the phases; refer to (2.4) and (2.5). Given $r_1(t)$ and $r_2(t)$, the optimal non-coherent decision rule for the data bit b_k is

$$\hat{b}_k = arg \max_{b=-1,+1} \left\{ p\left(a_1, \dot{a}_1, \dot{\psi}_1 \,|\dot{\theta} = \pi bh/T\right) \int_{-\infty}^{\infty} p\left(a_2, \dot{a}_2, \dot{\psi}_2 \,|\dot{\psi}_R\right) p\left(\dot{\psi}_R|\dot{\theta} = \pi bh/T\right) d\dot{\psi}_R \right\}, \tag{3.9}$$

where $\dot{\psi}_1$ and $\dot{\psi}_2$ are the derivatives of ψ_1 and ψ_2 respectively, $p\left(a_1, \dot{a}_1, \dot{\psi}_1 \,|\dot{\theta} = \pi bh/T\right)$ is the joint pdf of $a_1, \dot{a}_1, \dot{\psi}_1$ given the data phase derivative $\dot{\theta} = \pi bh/T$, and $p\left(a_2, \dot{a}_2, \dot{\psi}_2 \,|\dot{\psi}_R\right)$ is the joint pdf $a_2, \dot{a}_2, \dot{\psi}_2$ given the forwarded phase derivative $\dot{\psi}_R$, and $p\left(\dot{\psi}_R|\dot{\theta} = \pi bh/T\right)$ is the pdf of $\dot{\psi}_R$ given the data phase derivative $\dot{\theta} = \pi bh/T$. The pdf $p\left(a_1, \dot{a}_1, \dot{\psi}_1 \,|\dot{\theta} = \pi bh/T\right)$ is given by (2.22) after inclusion of the index "1". The pdf $p\left(a_2, \dot{a}_2, \dot{\psi}_2 \,|\dot{\psi}_R\right)$ is also given by the same equation, except for a change in indexing to "2" and the replacement of $\dot{\theta}$ by $\dot{\psi}_R$. As for the pdf $p\left(\dot{\psi}_R|\dot{\theta} = \pi bh/T\right)$, it is given by (2.24) after proper changes in indexing. The most important thing to realize at this point though is that, because of the integral and the forms of the two pdfs, the solution to the above optimal decoding metric is not mathematically tractable. For this reason, we treat the $S-R$ link as if it is ideal, i.e. replace $p\left(\dot{\psi}_R|\dot{\theta} = \pi bh/T\right)$ in the optimal decision rule

by an unit impulse function centered at $\dot{\psi}_R = \pi bh/T$, and adopt the suboptimal decision rule

$$\hat{b}_k = arg \max_{b=-1,+1} \left\{ p\left(a_1, \dot{a}_1, \dot{\psi}_1 \,|\dot{\theta} = \pi bh/T\right) p\left(a_2, \dot{a}_2, \dot{\psi}_2 \,|\dot{\psi}_R = \pi bh/T\right) \right\} \tag{3.10}$$

instead. As shown in Appendix B, this subpotimal decision rule simplifies to

$$\hat{b}_k = \text{sgn}\left(2\sum_{k=1}^{2} a_k^2 \dot{\psi}_k\right) = \text{sgn}\left(\sum_{k=1}^{2} D_k\right), \tag{3.11}$$

where

$$D_k = 2a_k^2 \dot{\psi}_k = 2\text{Im}\left(r_k^* \dot{r}_k^*\right) = \left(r_k^* \dot{r}_k\right) \begin{pmatrix} 0 & -j \\ j & 0 \end{pmatrix} \begin{pmatrix} r_k \\ \dot{r}_k \end{pmatrix}. \tag{3.12}$$

(3.11) clearly demonstrates that the detector first performs non-coherent combining before making the decision on the data. The weighting coefficients a_1^2 and a_2^2 in the combiner are due to the square amplitude terms inside the second exponential functions of the PDFs $p\left(\dot{\psi}_R|\dot{\theta} = \pi bh/T\right)$ and $p\left(\dot{\psi}_R|\dot{\psi}_R = \pi bh/T\right)$; refer to Appendix B.

It should be pointed out that not only do we adopt (3.11) for the proposed PF scheme, we also apply it to DF as well.

3.2 Performance Analysis

3.2.1 Phase-Forward

The BEP of the detector in (3.11) can be obtained via the characteristic function (CF) approach described in [28]. Without loss of generality, we assume the data bit equals $+1$ (i.e. $\dot{\theta} = \pi h/T$). Consequently, the detector in (3.11) makes a wrong decision when $D = D_1 + D_2 < 0$.

First, we observe from (3.4) that when $\theta(t)$ is given, $r_1(t)$ is a complex Gaussian random process because $g_1(t)$ and $n_1(t)$ are independent Gaussian random processes. Therefore, $\mathbf{R}_1 = (r_1 \dot{r}_1)^T$ is a complex Gaussian vector when conditioned on the data phase θ. The same is true for $\mathbf{R}_2 = (r_2 \dot{r}_2)^T$ when conditioned on the relay phase ψ_0 (or $\hat{\theta}$ in the case of DF); refer to (3.6). Consequently, the terms $D_1 = \mathbf{R}_1^\dagger \mathbf{F} \mathbf{R}_1$ and $D_2 = \mathbf{R}_2^\dagger \mathbf{F} \mathbf{R}_2$, $\mathbf{F}$ being the 2×2 matrix in (3.12), are both quadratic forms of complex Gaussian variates. The covariance matrices of the Gaussian vectors $\mathbf{R_1}$ and $\mathbf{R_2}$ are

$$\phi_k = \tfrac{1}{2} E\left[\mathbf{R}_k \mathbf{R}_k^\dagger\right] = \begin{pmatrix} \alpha_k^2 & -j\chi_k^2 \\ j\chi_k^2 & \beta_k^2 \end{pmatrix}, \qquad k = 1,2, \tag{3.13}$$

where $\alpha_1^2, \beta_1^2, \chi_1^2$ are determined from (2.21) by adding the index "1" associated with the $S-D$ link, and $\alpha_2^2, \beta_2^2, \chi_2^2$ are determined from the same equation by adding the index "2" associated with the $R-D$ link and by replacing the term $\dot{\theta}$ by $\dot{\psi}_R$.

From [28], the characteristic function of D_k is

$$\varphi_k(s) = E\left[e^{sD_k}\right] = \|\mathbf{I} + 2s\phi_k \mathbf{F}\|^{-1} = \frac{p_{k,1} p_{k,2}}{(s - p_{k,1})(s - p_{k,2})}, \qquad k = 1,2, \tag{3.14}$$

where s is the transform domain variable, $\mathbf{I}$ is a 2×2 identity matrix, $\|\cdot\|$ represents determinant, and

$$\begin{aligned} p_{k,1} &= -\left(2\alpha_k \beta_k (1 + \rho_k)\right)^{-1} < 0 \\ p_{k,2} &= +\left(2\alpha_k \beta_k (1 - \rho_k)\right)^{-1} > 0 \end{aligned} \tag{3.15}$$

are respectively the left and right plane poles of $\varphi_k(s)$. Since fading and noise in the $S-D$ and the $R-D$ links are statistically independent, the CF of the decision variable $D = D_1 + D_2$ is simply $\varphi(s) = \varphi_1(s)\varphi_2(s)$. The probability of $D < 0$ is the negative sum of the residues of $\varphi(s)/s$ at the right plane poles $p_{1,2}$ and $p_{2,2}$ [28]. If these poles are distinct,

i.e. $p_{1,1} \neq p_{2,1}$ and $p_{1,2} \neq p_{2,2}$, then

$$\Pr[D<0|\dot{\psi}_0] = \frac{-p_{1,1}}{p_{1,2}-p_{1,1}} \cdot \frac{p_{2,1}p_{2,2}}{(p_{1,2}-p_{2,1})(p_{1,2}-p_{2,2})} + \frac{-p_{2,1}}{p_{2,2}-p_{2,1}} \cdot \frac{p_{1,1}p_{1,2}}{(p_{2,2}-p_{1,1})(p_{2,2}-p_{1,2})} \tag{3.16}$$

$$(p_{1,1} \neq p_{2,1} \ \ and \ \ p_{1,2} \neq p_{2,2}).$$

On the other hand if $p_{1,1} = p_{2,1}$ and $p_{1,2} = p_{2,2}$, then

$$\Pr[D<0|\dot{\psi}_0] = \left(\frac{-p_{1,1}}{p_{1,2}-p_{1,1}}\right)^2 \cdot \left(1+\frac{p_{1,2}}{p_{1,2}-p_{1,1}}\right) \tag{3.17}$$

$$(p_{1,1} = p_{2,1} \quad \text{and} \quad p_{1,2} = p_{2,2}).$$

We emphasize that (3.16) and (3.17) are conditional error probabilities. To obtain the unconditional error probability P_b, we take the average of $\Pr[D<0|\dot{\psi}_0]$ over the pdf of $\dot{\psi}_0$. Once again, this pdf can be determined from (2.24) by adding the index "0" associated with $S-R$ link:

$$p(\dot{\psi}_0|\dot{\theta} = \pi h/T) = \frac{\beta_0^2(1-\rho_0^2)}{2\alpha_0^2}\left[\left(\dot{\psi}_0 - \rho_0\frac{\beta_0}{\alpha_0}\right)^2 + \frac{\beta_0^2}{\alpha_0^2}\left(1-\rho_0^2\right)\right]^{-3/2}. \tag{3.18}$$

The terms $\alpha_0^2, \beta_0^2, \chi_0^2, \sigma_{\dot{n}}^2, \lambda_0, \rho_0$ in the above equation are similarly obtained from (2.21). The unconditional BEP of PF is

$$P_b = \int_{-\infty}^{\infty} \Pr[D<0|\dot{\psi}_0] p(\dot{\psi}_0|\dot{\theta} = \pi h/T) d\dot{\psi}_0, \tag{3.19}$$

which is semi-analytical.

3.2.2 Decode-and-Forward

For conventional DF, the BEP at the destination can be expressed in closed-form as

$$\begin{aligned} P_b &= \Pr\left[D<0|\hat{\dot{\theta}} = \dot{\theta}\right] \Pr(\dot{\psi}_0 > 0|\dot{\theta} = \pi h/T) \\ &+ \Pr\left[D<0|\hat{\dot{\theta}} = -\dot{\theta}\right] \Pr(\dot{\psi}_0 < 0|\dot{\theta} = \pi h/T), \end{aligned} \tag{3.20}$$

where $\Pr(\dot{\psi}_0 < 0 | \dot{\theta} = \pi h/T)$ is the probability of making a wrong decision at the relay, and $\Pr\left[D < 0 | \hat{\dot{\theta}} = \dot{\theta}\right]$, $\Pr\left[D < 0 | \hat{\dot{\theta}} = -\dot{\theta}\right]$ are probabilities of making a wrong decision at the final destination after the relay makes a correct/erroneous decision. The latter two probabilities can be easily obtained from (3.16) and (3.17) by simply replacing $\dot{\psi}_0$ in these equations by $\dot{\theta}$ and $-\dot{\theta}$ respectively, Furthermore, the bit error probability of the relay detector can be shown equal to

$$\Pr(\dot{\psi}_0 < 0 | \dot{\theta} = \pi h/T) = \frac{-p_{0,1}}{p_{0,2} - p_{0,1}}, \tag{3.21}$$

where

$$\begin{aligned} p_{0,1} &= -\left(2\alpha_0\beta_0(1+\rho_0)\right)^{-1} < 0 \\ p_{0,2} &= +\left(2\alpha_0\beta_0(1-\rho_0)\right)^{-1} > 0 \end{aligned}, \tag{3.22}$$

with $\alpha_0, \beta_0, \rho_0$ as defined in (2.21) by adding the index "1" designated for the $S-D$ link to the general equations. The results in (3.21) and (3.22) are a direct consequence of the fact that the detector in a DF relay is a (single-channel) quadratic detector.

3.3 Simulation Results and Discussion

We present in this section analytical and simulation results for the BEP of the proposed PF non-coherent CPFSK cooperation scheme as a function of the $S-D$ link's SNR

$$SNR_1 = \frac{\gamma_1}{\sigma_n^2} = \frac{\gamma_1 T}{N_0 BT} = \frac{E_1}{N_0(BT)}, \tag{3.23}$$

where γ_1 and $\sigma_n^2 = N_0 B$ are the fading and noise variances defined in (2.1) and (2.2) respectively, BT is the normalized bandwidth of the CPFSK signal in Table 2.1, and E_1/N_0 is the bit-energy to noise power density ratio. Traditionally, the BEP of a modulation scheme is "measured" against E_1/N_0. This is especially important when we wish to

compare modulation schemes with different bandwidths. In this investigation though, the focus is more on comparing different forwarding strategies given a modulation scheme, so it is fine to measure BEP as a function of SNR_1.

In general, this SNR will be different from that in the $S-R$ link, $\text{SNR}_0 = \gamma_0/\sigma_n^2$, and that in the $R-D$ link $\text{SNR}_2 = \gamma_2/\sigma_n^2$. These differences in SNR are attributed to the unequal separations betweens the pairs of nodes. The source and the relay, however, are actually transmitting at the same power level; refer to (3.3), (3.6), and (3.1). Unless otherwise stated, the results shown in any graph are for the case of equally strong links. The Doppler frequencies in the three links are always identical, i.e. $f_1 = f_2 = f_3 = f_D$.

In the simulation, we generated sampled MSK signals at a rate of 16 samples per bit interval. Fading samples are generated by the filtering method, in conjunction with interpolation. The discrete-time faded CPFSK signal, together with additive white Gaussian noise, are fed to a digital brick-wall filter whose bandwidth is set according to Table 2.1. This set up (as oppose to one that adds the faded CPFSK signal directly to a band-limited Gaussian noise) is essential to verify the correctness of the noise-bandwidth used in the analysis. This stems from the fact that any practical CFPSK receiver can not limit the noise bandwidth without introducing some distortion to the signal at the same time. The analytical model, on the hand, assumes no such distortion. In the simulation, data decisions are made at the mid-symbol positions.

3.3.1 99.9% Bandwidth

We first consider the performance of the proposed cooperative PF CPFSK system with a destination receiver designed based on the 99.9% bandwidth of the underlying CPFSK

signal; refer to Table 2.1. We further classify the results into static fading and time-selective fading.

3.3.1.1 Static Fading

We first show in Fig. 3.2 analytical BEP results for CPFSK modulation with static fading and different modulation index h. Only direct transmission without cooperation is considered in this figure. It is observed that in general, the larger the modulation index h, the lower the BEP. Note however that the bandwidth of CPFSK also increases with the modulation index h; refer to Table 2.1.

We next show in Fig. 3.3 analytical BEP results for MSK (CPFSK with $h = 1/2$) with static fading and equally strong links. It is observed that the BEP of the proposed PF scheme decreases at a rate slightly greater than inverse SNR_1, and at a BEP of 10^{-4}, it is 2 dB more energy efficient than DF. As expected, the results in the figure show that at any given SNR_1, both PF and DF attain a lower BEP than no cooperation (5 dB more energy efficient at a BEP of 10^{-4}). However, we should be reminded that cooperation requires twice as much transmit power as no cooperation. Nonetheless, even with this 3 dB power difference taken into consideration, the proposed PF scheme still offers substantial improvement over no cooperation at large SNR. It is observed that while PF performs better than DF at high SNR, the opposite appears to be true at low SNR. The cross-over point is at 17 dB. As we are going to show later in Fig. 3.5, the simulated BEP of PF is always lower than DF. We will elaborate on this discrepancy later in the thesis.

Before plotting the BEP performance, we were expecting a second order diversity effect when we apply cooperation. However, in Fig. 3.3 we do not see much second order

diversity effect for both PF and DF, except in the range from 10 to 15 dB. The reason is because we assume the three links are equally strong, and therefore fading in $S-R$ link will destroy any hope of a second order diversity effect. For explanation sake, let us just consider decode-and-forward. The BEP at the relay is $P_b \propto 1/SNR$, where $SNR = SNR_1$ is the signal-to-noise ratio common to all three links. When the relay makes a wrong decision, it forwards a data bit that is of opposite polarity to the transmitted data bit. Given all three links are equally strong, then the destination receiver will see two equally strong but contradicting pieces of information. So the BEP in this case will be $1/2$. On the other hand, when the relay makes a correct decision, then the destination receiver will see two equally strong pieces of information with the same polarity this time. The BEP in this case is proportional to $1/SNR^2$. So the overall BEP is proportional to

$$P_b \times \frac{1}{2} + (1-P_b) \times \frac{1}{SNR^2} \approx \frac{1}{2SNR}, \tag{3.24}$$

which shows no diversity effect. The same argument can be applied to the proposed PF scheme as well.

The scenario which cooperation offers an overwhelming advantage over no cooperation is when the SNR in the $S-R$ link is substantially higher than that in the direct link. This scenario would occur when the relay is placed very close to the source, and with little obstacles between the two. We show in Fig. 3.4 analytical results for MSK with static fading and $\text{SNR}_0 = \text{SNR}_1 + 10\text{dB}$ and $\text{SNR}_0 = \text{SNR}_1 + 20\text{dB}$. The second-order diversity effect provided by the proposed PF scheme is very prominent in these asymmetric SNR cases. It is also observed that when SNR_0 is 20 dB higher than SNR_1, DF appears to be better than the proposed PF scheme. We will comment on this when we study the simulation results in the next few figures.

In Fig. 3.5, we check the accuracy of the analytical model (specifically the choice of the noise bandwidth) by comparing it against simulation. From the figure, we see that the analytical and simulation results for no cooperation and DF show excellent agreements. There is a small difference between simulation and analysis for PF. We suspect that the reason could be one or more of the following: our analysis result is semi-analytical and requires truncation of an infinite integral to a finite range; our analysis result is semi-analytical and requires numerical integration that can lead to quantization errors; in simulation we used lowpass filters to limit the amount of noise admitted into the receiver, but in analysis we did not consider filters, which will distort the CPM signal.

We also show in Fig. 3.6 the simulation results for amplify-and-forward. In this latter case, the forwarded signal assumes the form

$$\hat{s}(t) = r_0(t)/\sqrt{\gamma_0 + \sigma_n^2}, \qquad \text{(AF)} \tag{3.25}$$

where the scaling factor $\sqrt{\gamma_0 + \sigma_n^2}$ ensures that $E\left[|\hat{s}(t)|^2\right] = 1$, just like in PF and DF. In comparison with conventional AF, the proposed PF scheme has practically the same BEP performance in a static fading channel.

So far, the concept of Phase Forward is being introduced in the context of constant envelop modulation. The natural question to ask is: is PF applicable to linear modulation schemes like Phase Shift Keying (PSK). To answer this question, we show in Fig. 3.7 the simulation results for differential encoded and detected binary phase shift keying (DBPSK), for the case of no cooperation, and the case of cooperation with DF, PF and AF. The most interesting conclusion that can be drawn here is that the idea of PF is equally applicable to PSK. As in the case of CPFSK, the performance of PF in PSK is between that of conventional DF and AF. In comparing the DBPSK and CPFSK curves, we notice the

existence of a 6 dB gap. While the result may suggest that one should abandon CPFSK modulation altogether, we like to remind the reader that there are actually plenty of practical mobile radio systems that adopt constant envelop modulations (e.g. taxi, dispatch, GSM, Bluetooth, etc.). Besides, a large portion of this 6 dB gap can be reduced if we introduce an integrate-dump filter after discriminator detection. Fig. 3.8 shows the results of the proposed PF scheme when the soft decision variable $\sum_{k=1}^{2} D_k$ is taken 16 times per bit interval and then averaged over one symbol interval before applied to the decision rule in (3.11). The gap between DBPSK and CPFSK now reduces to 2 dB. While MSK is till less power efficient than BPSK, the reader is reminded again that MSK support the use of inexpensive non-linear power amplifiers.

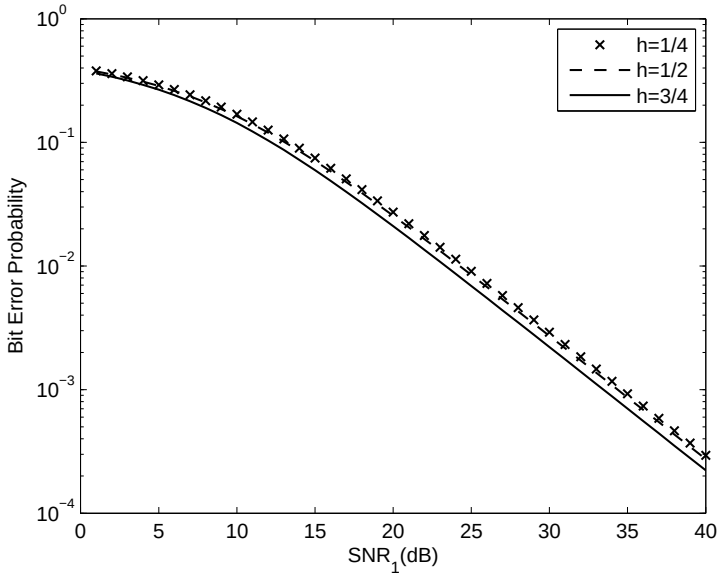

Figure 3.2: Analytical BEP of CPFSK with different modulation index h at $f_D T = 0$ with no cooperation

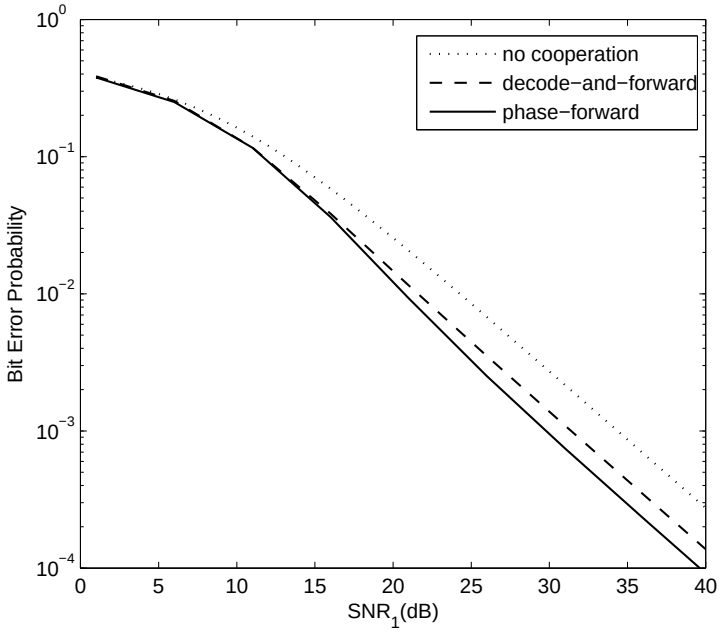

Figure 3.3: Analytical BEP of MSK at $f_D T = 0$; equally strong links.

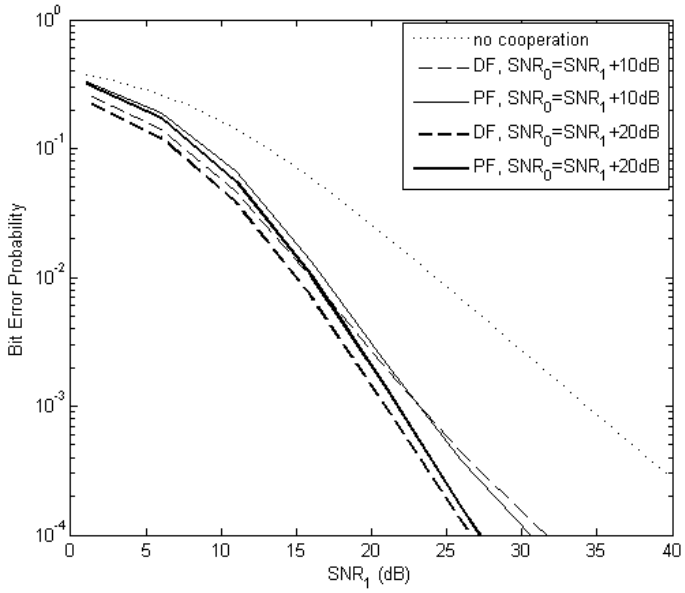

Figure 3.4: Effect of $S-R$ link's SNR on the BEP of MSK at $f_D T = 0$.

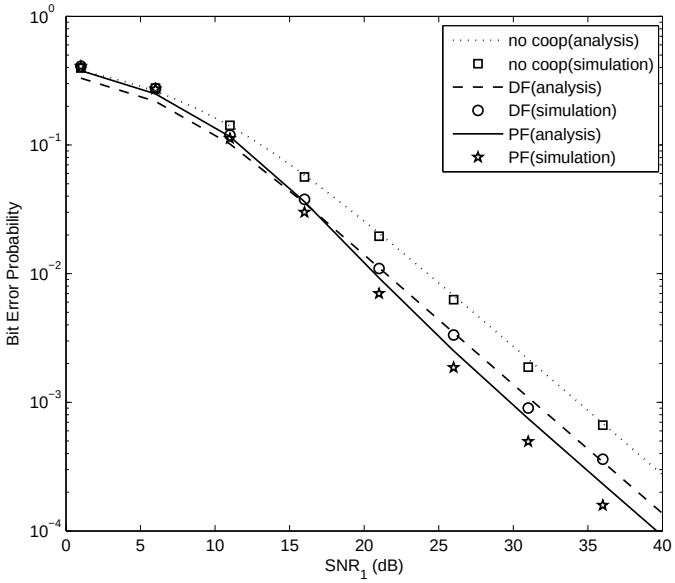

Figure 3.5: Comparison between analytical and simulation results for MSK at $f_D T = 0$; equally strong links.

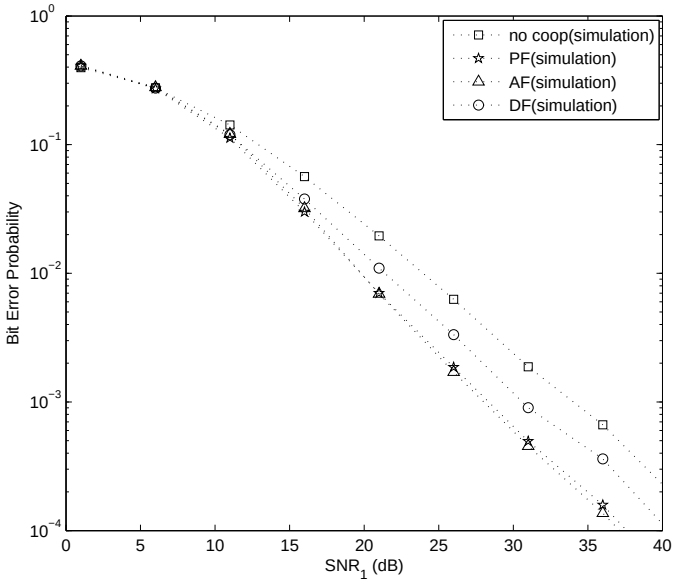

Figure 3.6: Comparison between no cooperation, DF, PF and AF for MSK at $f_D T = 0$; equally strong links.

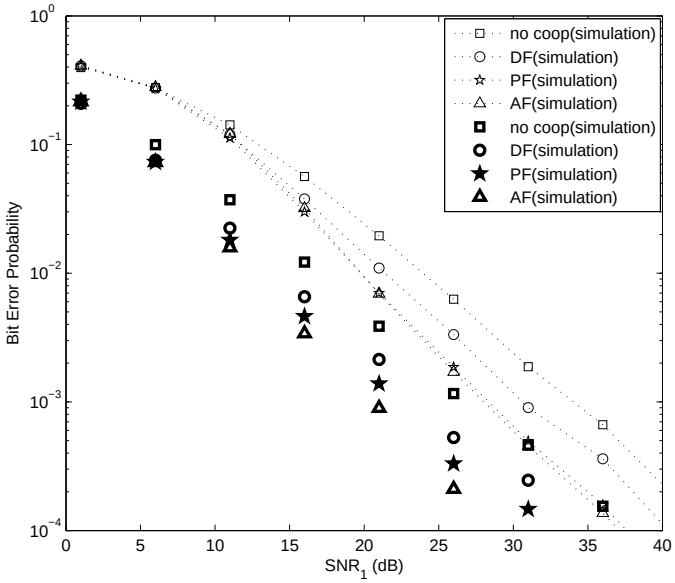

Figure 3.7: Comparison between differential encoded and detected binary phase shift keying and MSK at $f_D T = 0$; equally strong links.

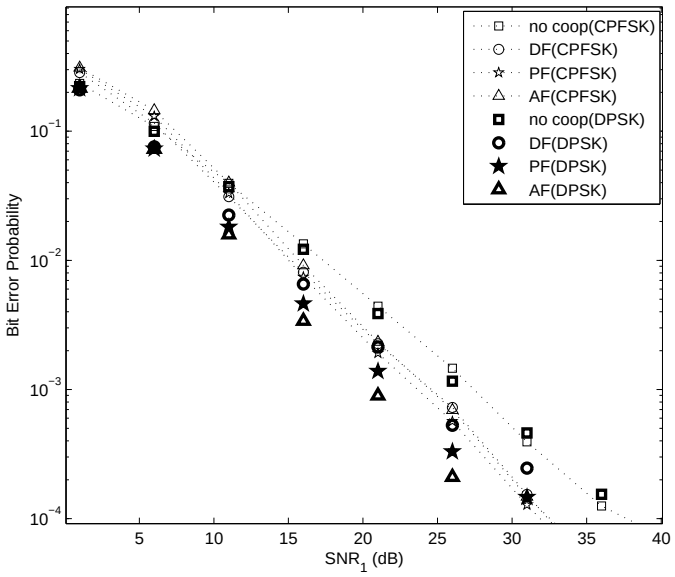

Figure 3.8: Comparison between DBPSK and MSK with post-detection integrate-and-dump filter; $f_D T = 0$, equally strong links.

3.3.1.2 Fast Fading

This section shows the result of the proposed PF scheme in "fast" fading environment.

First in Fig. 3.9 we show the BEP results for CPFSK with no cooperation. The doppler frequency in this figure is $fdT = 0.03$. This means the wireless terminal moves relatively fast. For example, for a carrier of 1.9GHz and data rate of 13Kbps, $fdT = 0.03$ corresponds to an actual doppler of 0.39KHz, and the terminal moves at a speed of 221km/h. From this figure we can see that in a fast fading environment there is an error floor, Similar to the static fading case though, the BEP improves with an increasing modulation index h.

In Fig. 3.10 we consider only MSK, i.e. h=1/2, but with different doppler frequencies. Again, the result is for no cooperation. From this figure we can see that the error floor increases with the doppler frequency.

In Fig. 3.11, we confirm the accuracy of the analytical model again (specifically the choice of the noise bandwidth) by comparing it against simulation. The doppler frequency is $fdT = 0.03$ and the three links are equally strong. From this figure, we see that the analytical and simulation results for no cooperation and DF show excellent agreements. However for the proposed PF scheme, the analytical results are found to be slightly pessimistic. As we described before, the CPFSK signal is not band-limited, so the use of the band-limited filter will distort the signal at the relay for PF scheme. This distortion will bring a higher error floor as we can see in the figure.

In Fig. 3.12 in a "fast" fading channel, simulation result shows that PF is worse than AF. The latter attain a strong second-order diversity effect at the expense of costly linear amplifiers to support non-constant-envelop transmission at the relay. Here we would like to mention that the phase-forward scheme only forwards the received phase at the relay to

the destination, and the fading amplitude information in the S-R link is lost in the process. In a fast fading channel, fading in the S-R link changes quickly, so losing the amplitude information would lead to worse performance.

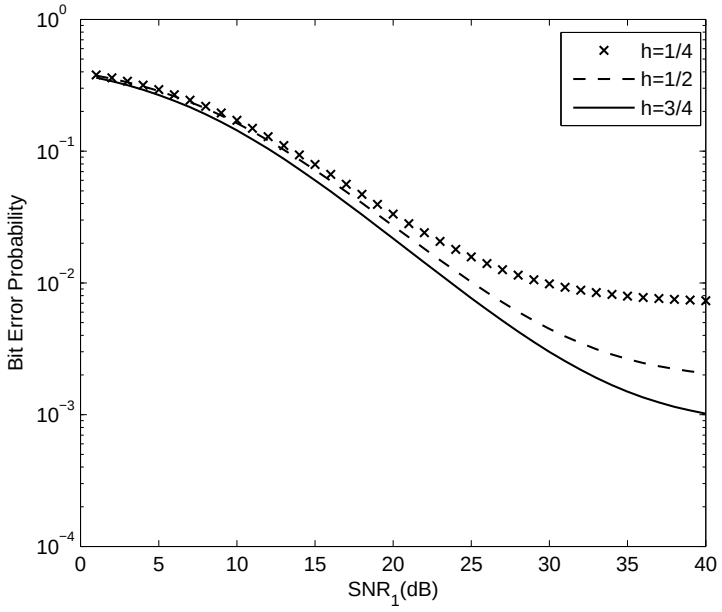

Figure 3.9: Analytical BEP of CPFSK with different modulation index h at $f_D T = 0.03$ with no cooperation.

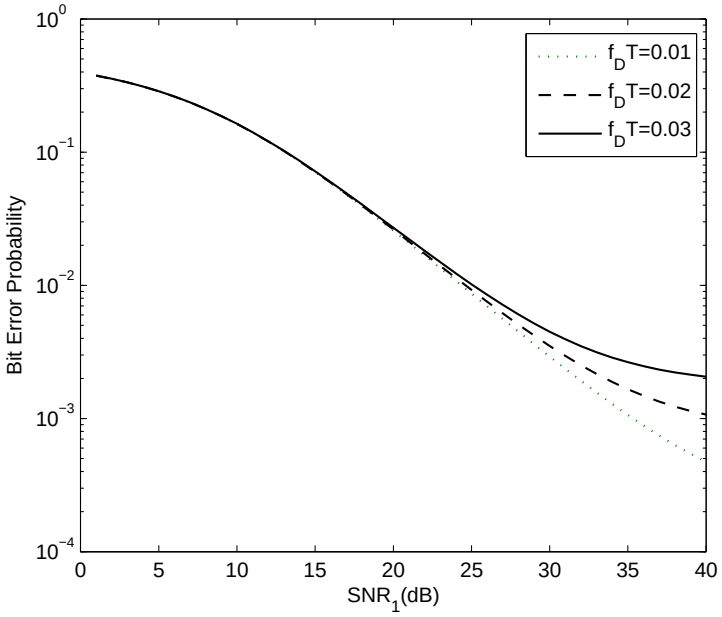

Figure 3.10: Analytical BEP of MSK for different doppler frequency with no cooperation.

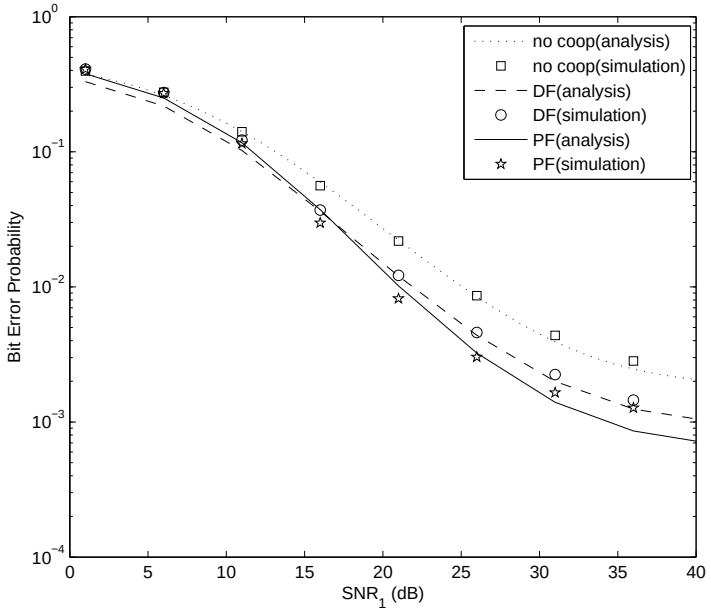

Figure 3.11: Comparison between analytical and simulation results for MSK at $f_D T = 0.03$; equally strong links.

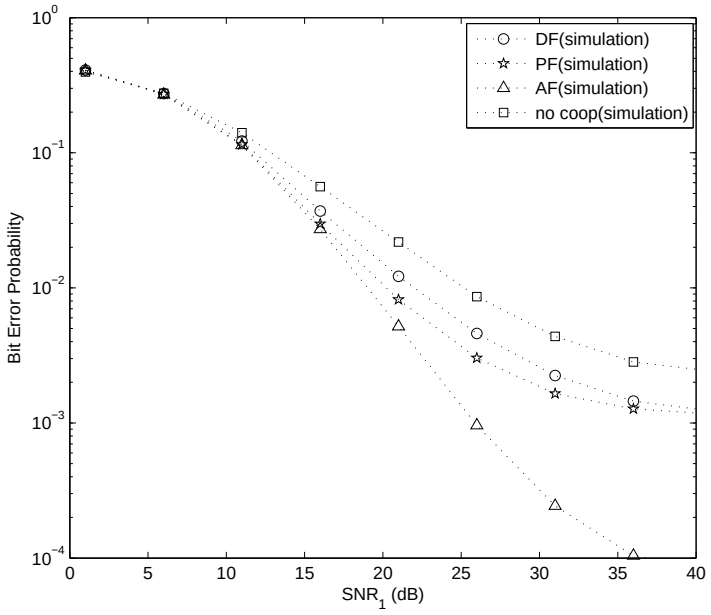

Figure 3.12: Comparison between no cooperation, DF, PF and AF for MSK at $f_D T = 0.03$; equally strong links.

3.3.2 99% Bandwidth

The results we have seen so far are for a destination receiver designed based on the 99.9% bandwdith of the underlying CPFSK signal. In this section we show both analytical and simulation results for the proposed PF scheme with a receiver designed based on 99% bandwidth of the CPFSK signal in Table 2.1. Again, the results are categorized according to whether fading is static or not.

3.3.2.1 Static Fading

We first show in Fig. 3.13 analytical BEP results for MSK (CPFSK with $h = 1/2$) with static fading and equally strong links. Comparing with Fig. 3.3, we observe that the BEP results for PF, DF, and no cooperation based on the 99% bandwidth are consistently 5 dB more efficient than the corresponding results based on the 99.9% bandwidth. Furthermore, if we compare the 99% and 99.9% bandwidth results based on E_1/N_0 instead of SNR_1, then there will be an additional 3.6 dB gain in power efficiency; refer to (3.23).

Fig. 3.14 shows again the BEP result for MSK with static fading but here we consider the SNR in $S-R$ link to be higher than those in the other two links. Comparing with Fig. 3.4 we find that the 99% bandwidth BEP result is better than the 99.9% case, and a second order diversity effect is observed.

In Fig. 3.15 we check the accuracy of the analytical results obtained under the 99% bandwidth assumption by comparing them against simulation. From the figure, we can see the two sets of results show good agreement. We also show in this figure the simulation result for AF. It is observed that AF and PF have very similar performance under static fading and 99% bandwidth.

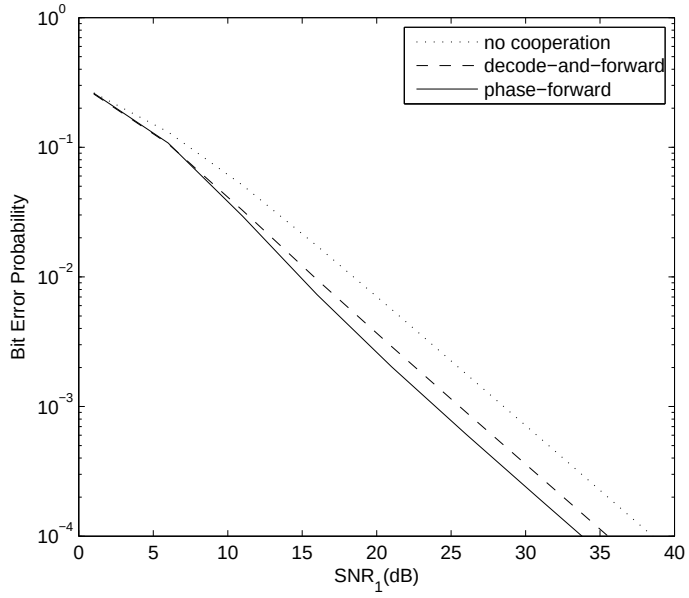

Figure 3.13: Analytical BEP of MSK at $f_D T = 0$; equally strong links.

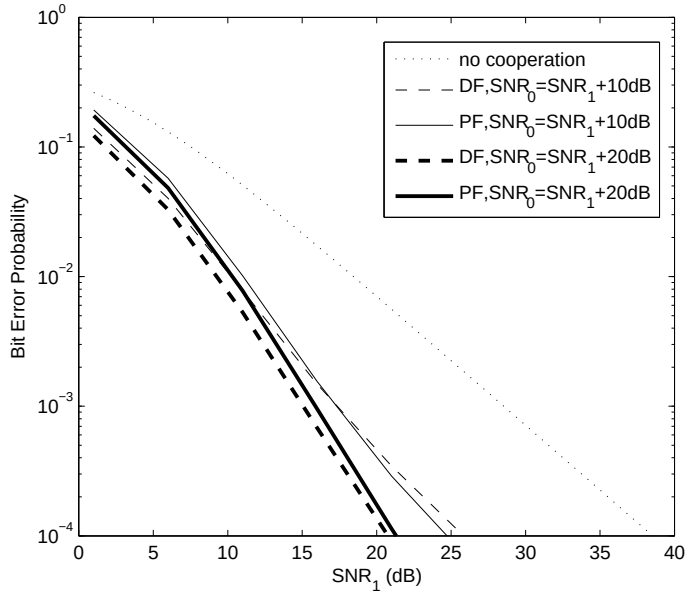

Figure 3.14: Effect of $S-R$ link's SNR on the BEP of MSK at $f_D T = 0$.

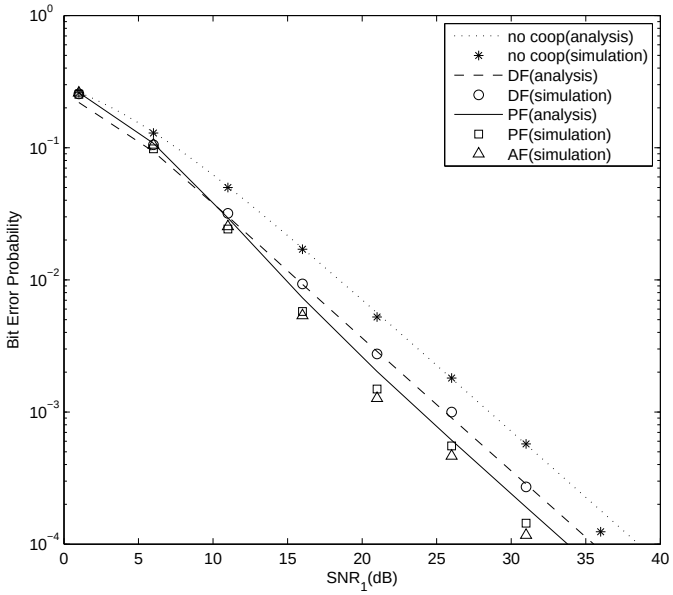

Figure 3.15: Comparison between analytical and simulation results for MSK at $f_D T = 0$; equally strong links and no antenna selection.

3.3.2.2 Fasting Fading

Fig. 3.16 is a repeat of Fig. 3.15 except that we now consider a "fast" fading channel with a normalized Doppler frequency of $f_D T = 0.03$. From this figure, we see that the analytical and simulation results for no cooperation and DF show excellent agreements. However for the proposed PF scheme, the analytical results are found to be slightly pessimistic.

As in Fig. 3.12, we found that PF is worse than AF. The latter attain a strong second-order diversity effect at the expense of costly linear amplifiers to support non-constant-envelop transmission at the relay.

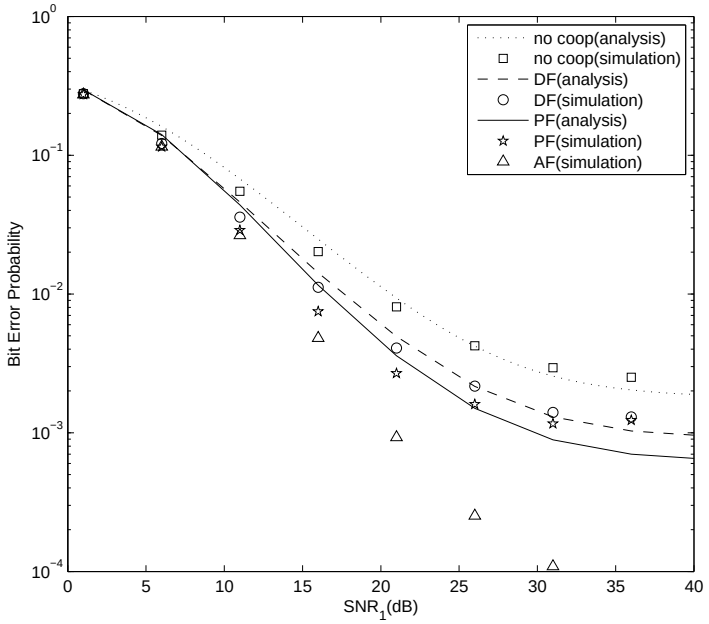

Figure 3.16: Comparison between analytical and simulation results for MSK at $f_D T = 0.03$; equally strong links and no antenna selection.

Chapter 4

Phase Forward Cooperative Communications with Antenna Selection and Continuous Phase Modulation

From Chapter 3 we observe that the system we proposed would benefit from cooperative transmission. Furthermore, we also concluded that the proposed phase-forward scheme have better performance than the conventional decode-and-forward scheme if the signal-to-noise ratio is reasonably high, and second order diversity can be achieved when the source-to-relay link is stronger than the other two links. In this chapter we propose two extensions to the Phase Forward (PF) relaying strategy for cooperative communication. One extension is the replacement of CPFSK modulation by Gaussian filtered Minimum Shift Keying (GMSK) modulation. The second extension is the incorporation of antenna selection at the relay. As in Chapter 3, we first analyze the performance of the proposed system with GMSK modulation and the dual-antenna selection, and then compare the analytical results

with simulation results.

4.1 GMSK and Phase-Forward

As stated in Section 2.2.2, GMSK uses a smooth frequency pulse. As a result, it has a more compact power spectrum than CPFSK. As a matter of fact, GMSK and its variants have been adopted in a number of standards, including Blutetooth. In this section, we will analyze the BEP of GMSK when used in a cooperative communication system with a phase-forward relay. The resulting scheme will be referred to as PF-GMSK

4.1.1 BEP Analysis

Consider (2.12) and (2.14) again. The derivative of the transmitted signal phase in the two cases are

$$\dot{\theta}(t) = \frac{\pi h}{T} \sum_{k=-\infty}^{\infty} b_k \,\mathrm{rect}(t - kT), \qquad (CPFSK) \tag{4.1}$$

and

$$\dot{\theta}(t) = \frac{\pi h}{T} \sum_{n=-\infty}^{\infty} b_n p(t - nT), \qquad (GMSK) \tag{4.2}$$

where rect(t) is a unit-amplitude rectangular pulse time-limited to the interval [0,T] and $p(t)$ is the Gaussian pulse defined in (2.14). Since the pulse $p(t)$ is strictly speaking infinitely long, therefore, $\dot{\theta}(t)$ in (4.2) depends on both the current data symbol b_k as well as previous and "future" data symbols $b_{-\infty}, \cdots b_{k-1}, b_{k+1}, \cdots b_{\infty}$. Since $p(t)$ centers at $t = 0$, so data decisions will be made at t=nT. Without loss of generality, lets consider the detection of the data bit b_0 and a decision instant of $t = 0$. Evaluating the data phase derivative $\dot{\theta}(t)$

at $t = 0$ under the conditions that $b_0 = 1$ and $h = 1/2$ yields [25]

$$\dot{\theta}(0) = \frac{\pi}{2T}\left[p(0) + \sum_{\substack{n=-\infty \\ n\neq 0}}^{\infty} b_n p(nT)\right], \tag{4.3}$$

where $(\cdots, b_{-3}, b_{-2}, b_{-1}, b_1, b_2, b_3, \cdots)$ represents intersymbol interference (ISI). Let the received signal phase at relay be ψ_0. The pdf of the corresponding phase derivative $\dot{\psi}_0$, given that $b_0 = +1$, is denoted as

$$\begin{aligned} p(\dot{\psi}_0|b_0 = +1) &= p(\dot{\psi}_0|b_0 = 1, b_1, b_{-1}, b_2, b_{-2}\cdots) \\ &= p\left(\dot{\psi}_0|\dot{\theta}(0) = \pi/(2T)\cdot(p(0) + \textstyle\sum_{n=-\infty}^{\infty} b_n p(nT)\right) \end{aligned}. \tag{4.4}$$

In Chapter 2, we showed that $p(t)$ is approximately limited time. This means the ISI in (4.4) can be truncated to a finite number of terms. Assuming there are $M = 2^m$ such ISI patterns, with the m-th pattern generating a phase derivative of $\dot{\theta}_m$. Then we can rewrite (4.2) in the form

$$p(\dot{\psi}_0|b_0 = +1) = \frac{1}{M}\sum_{m=1}^{M} p(\dot{\psi}_0|\,\dot{\theta}_m), \tag{4.5}$$

where $\dot{\theta}_m$ is the m-th linear combination of the $p(nT)'s$ of the form

$$\frac{\pi}{2T}\left[p(0) \pm p(T) \pm p(-T) \pm p(2T) \pm p(-2T)\cdots\right], \tag{4.6}$$

and $1/M$ is the probability of any of the combinations. In this thesis we consider there are $M = 2^6$ possibilities and this is referred to as the GMSK-6 scheme in the literature. Finally the BEP of PF-GMSK without antenna selection can be written as

$$P_b = \frac{1}{M}\sum_{m=1}^{M}\int_{-\infty}^{\infty} \Pr[D < 0|\dot{\psi}_0]\, p(\dot{\psi}_0|\dot{\theta}_m)\, d\dot{\psi}_0, \tag{4.7}$$

where $p(\dot{\psi}_0|\dot{\theta}_m)$ takes on the same form as (3.18), except that the statistical parameters α_0, β_0, and ρ_0 in that equation (see (2.21) for the detailed definitions) are now derived

from $\dot{\theta} = \dot{\theta}_m$ instead of $\dot{\theta} = \pi h/T$. (4.7) is the semi-analytical expression for the BEP of PF-GMSK without antenna selection.

As for the BEP of GMSK with decode-and-forward, we can modify (3.20) to

$$P_b = \frac{1}{M}\sum_{m=1}^{M}\left(\Pr\left[\mathrm{D}<0|\hat{\dot{\theta}}=\dot{\theta}_{\mathrm{m}}\right]\Pr(\dot{\psi}_0>0|\dot{\theta}_{\mathrm{m}}) + \left(1-\Pr\left[\mathrm{D}<0|\hat{\dot{\theta}}=\dot{\theta}_{\mathrm{m}}\right]\right)\Pr(\dot{\psi}_0<0|\dot{\theta}_{\mathrm{m}})\right), \tag{4.8}$$

where $\dot{\theta}_m$ was defined in (4.6), $\Pr(\dot{\psi}_0 > 0|\,\dot{\theta}_m)$ and $\Pr(\dot{\psi}_0 < 0|\,\dot{\theta}_m)$ are the probabilities that the relay makes a correct and wrong decision respectively, and $\Pr\left[\mathrm{D}<0|\hat{\dot{\theta}}=\dot{\theta}\right]$ is the probability that the destination receiver makes a wrong decision after the relay makes correct decisions on all the data symbols. It should be pointed out that (4.8) is only an approximation of the BEP of GMSK with decode-and-forward. This stems from the fact that $\Pr\left[\dot{\psi}_0>0|\dot{\theta}_m\right]$ only gives us the probability that the main symbol is being detected correctly at the relay. Some interfering symbols will be detected correctly with the main symbol, and some detected erroneously. On the other hand, in calculating the probability $\left[D<0|\hat{\dot{\theta}}=\dot{\theta}_m\right]$, we implicitly assumes that the main and the interfering symbols are all detected correctly at the relay.

4.1.2 Simulation Results

We present in this section the BEP performance of the proposed PF-GMSK scheme in Rayleigh fading channels. All the results are based on GMSK-6 and a receiver with an ideal noise-limiting filter with a bandwidth of $BT = 0.91$, the 99% bandwidth of this GMSK signal. As in the previous chapter, the BEP will be plotted against the $S-D$ link's SNR, defined as $\mathrm{SNR}_1 = \gamma_1/\sigma_n^2$. In general, this SNR will be different from that in the $S-R$ link, $\mathrm{SNR}_0 = \gamma_0/\sigma_n^2$, and that in the $R-D$ link $\mathrm{SNR}_2 = \gamma_2/\sigma_n^2$. These differences in SNR are

attributed to the unequal separations betweens the pairs of nodes. The source and the relay, however, are actually transmitting at the same power level; refer to (2.11), (3.6), and (3.1). Unless otherwise stated, the results shown in any graph are for the case of equally strong links.

We first show in Fig. 4.1 analytical results for GMSK with no cooperation. Similar to the BEP result of CPFSK, the bit error probability increases with the Doppler frequency. Just like CPFSK, GMSK also has irreducible error floor under fast fading, but this error floor disappears under static fading.

In Fig. 4.2 the analytical BEP results for PF-GMSK, DF-GMSK, and no cooperation in a static fading enviornment, i.e. $f_D T = 0$, are shown. From the figure we can see that both DF and PF have better performance than no cooperation. In the PF case, the improvement is more than 4 dB. So even if we take into account that PF requires twice as much total energy than no-cooperation, there is still a considerable net performance improvement. In comparing PF with DF, we see the former provides a 2 dB improvement in energy efficient at a BEP of 10^{-4}.

Fig. 4.3 is almost the same as Fig. 4.2 except that in this figure we consider "fast" fading with an $f_D T = 0.03$. In this environment, PF still performs better than DF, and the irreducible error of PF is lower than that of DF. The reason is that DF essentially performs quantization at the relay, which leads to information loss. PF, on the other hand, does not involve quantization.

Although we see in Fig. 4.2 and Fig. 4.3 that both PF and DF perform better than no cooperation, none exhibits a second order diversity effect. As in the case of CPFSK, the reason is because the $S-R$, $R-D$ and $S-D$ links are equally strong links We show in Fig.

4.4 the BEP results for both PF and DF when the SNR in the $S-R$ link is higher than those in the two other links. From this figure, we can see that when the SNR in the $S-R$ link is 10 dB higher than the other two links, the PF and DF curves drop much faster than the no cooperation curve for SNR from 5 dB to 20 dB. Furthermore, if the SNR in the $S-R$ link is 20 dB higher than the other two links, we can see a very clear second order diversity effect for both PF and DF. Since the relay would indeed be close to the base station in practice, we believe this strong second order diversity effect indicated in this figure is realizable. The results in the figure appear to suggest that when the $S-R$ link is exceptionally strong, DF is actually slightly better than the proposed PF strategy. As we pointed out earlier though, the BEP analysis of DF-GMSK is only an approximation, as it implicitly assumes that the decoding relay makes correct decision not only on the main symbol, but also on the interfering symbols.

In Fig. 4.5 we show the analytical results for both GMSK and MSK with static fading and equally strong links. It is observed that MSK is 2 dB more power-efficient than GMSK at high SNR. Recall that GMSK pulse shaping introduces intersymbol interference whereas there is no such ISI in the MSK pulse. If we compare them based on the same E_1/N_0 as per (3.23), then we have to account for their bandwidth difference. Since MSK and GMSK have normalized 99% bandwidths of 1.18 and 0.91 respectively, the 2 dB advantage of MSK over GMSK needed to be reduced by $10*log(1.18/0.91) = 1.12$ dB when we compared them based on E_1/N_0.

Fig. 4.6 compares the analytical BEP of GMSK and MSK with fast fading and equally strong links. Again we see that MSK is more power-efficient than GMSK and has a lower error floor.

In Fig. 4.7 and Fig. 4.8 we confirm the accuracy of the analytical model for PF-GMSK by comparing it against simulation. We also show in these figures the simulation result for amplify-and-forward. In this latter case, the forwarded signal assumes the form

$$\hat{s}(t) = r_0(t)/\sqrt{\gamma_0 + \sigma_n^2}, \qquad \text{(AF)} \tag{4.9}$$

where the scaling factor $\sqrt{\gamma_0 + \sigma_n^2}$ ensures that $E\left[|\hat{s}(t)|^2\right] = 1$, just like in PF and DF. In the simulation, we generated sampled GMSK signals at a rate of 16 samples per bit interval. Fading samples are generated by the filtering method, in conjunction with interpolation. The discrete-time faded GMSK signals, together with additive white Gaussian noise, are fed to a digital brick-wall filter whose bandwidth is set to the 99% bandwidth of the GMSK signal. From the figures, we see that the analytical and simulation results for no cooperation and DF show good agreements. However for the proposed PF scheme, the analytical results are found to be slightly pessimistic. In comparison with conventional AF, the proposed PF scheme has practically the same BEP performance in a static fading channel (Fig. 4.7). However in a "fast" fading channel (Fig. 4.8), PF is noticeably worse than AF. The latter attain a noticeable diversity effect at the expense of costly linear amplifiers to support non-constant-envelop transmission at the relay. We can recover this loss through antenna selection at the relay. This is discussed next.

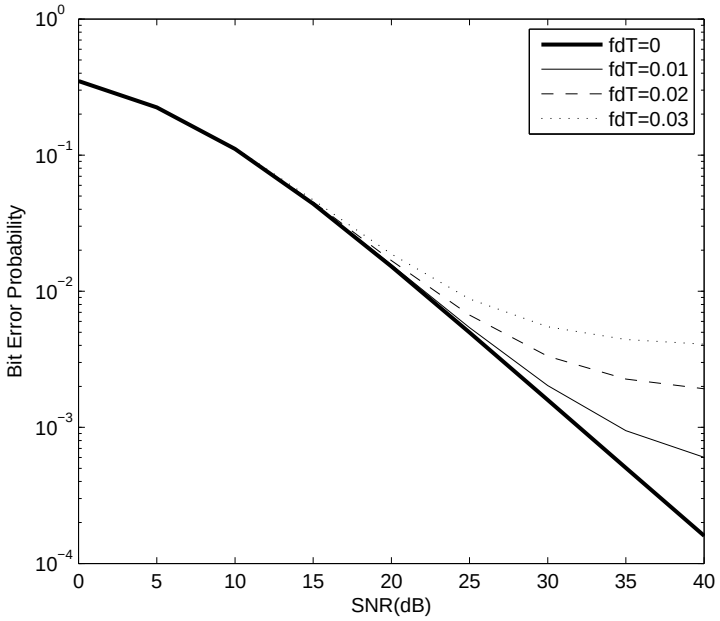

Figure 4.1: Analytical results for GMSK with different $f_D T$ and no cooperation.

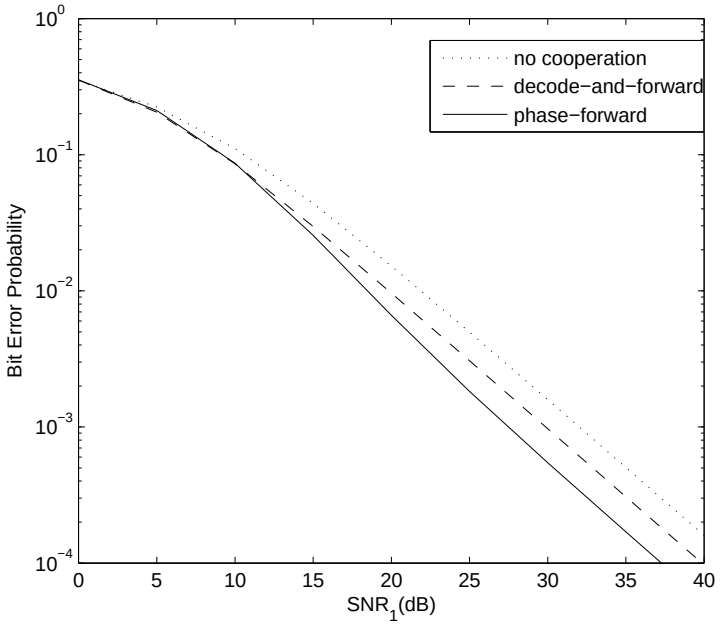

Figure 4.2: Analytical BEP of GMSK at $f_D T = 0$; equally strong links.

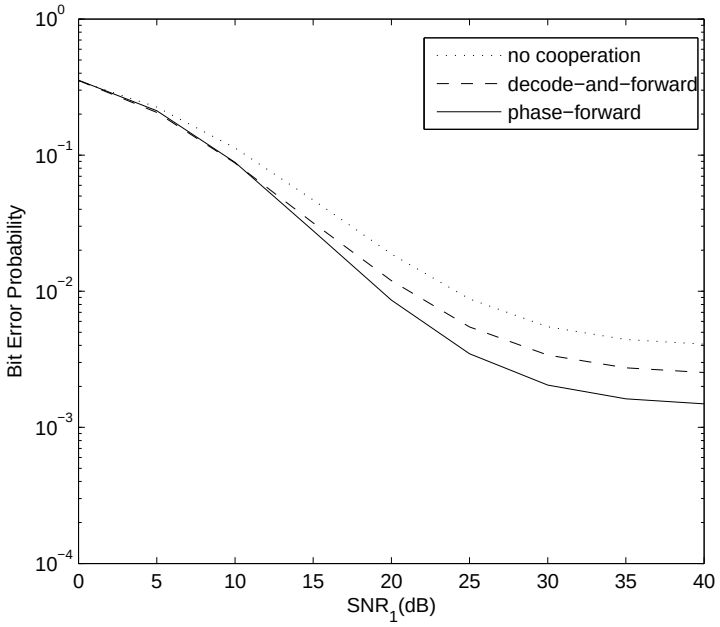

Figure 4.3: Analytical BEP of GMSK at $f_D T = 0.03$; equally strong links.

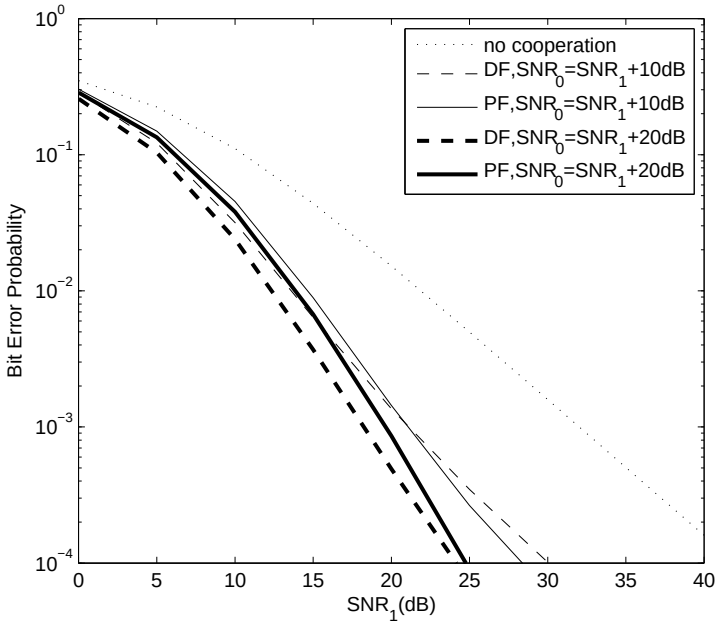

Figure 4.4: effect of $S-R$ link's SNR on the BEP of GMSK at $f_D T = 0$.

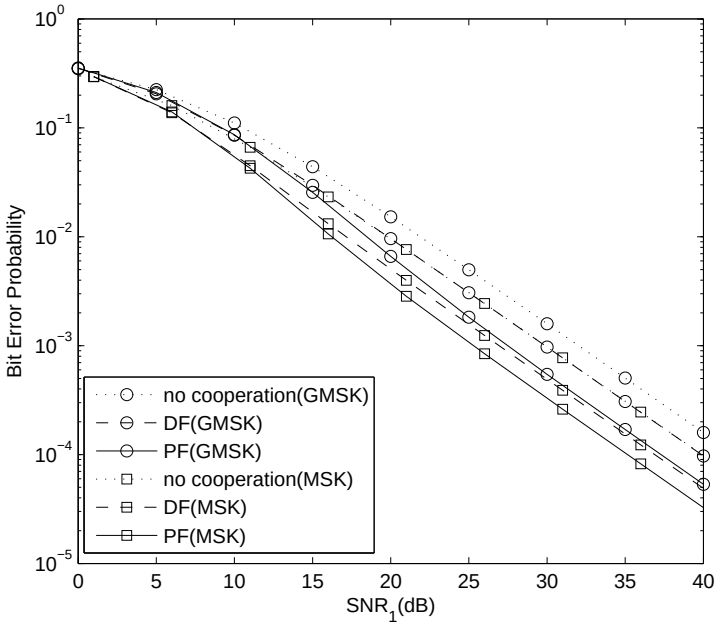

Figure 4.5: Analytical results for GMSK and MSK at $f_D T = 0$.

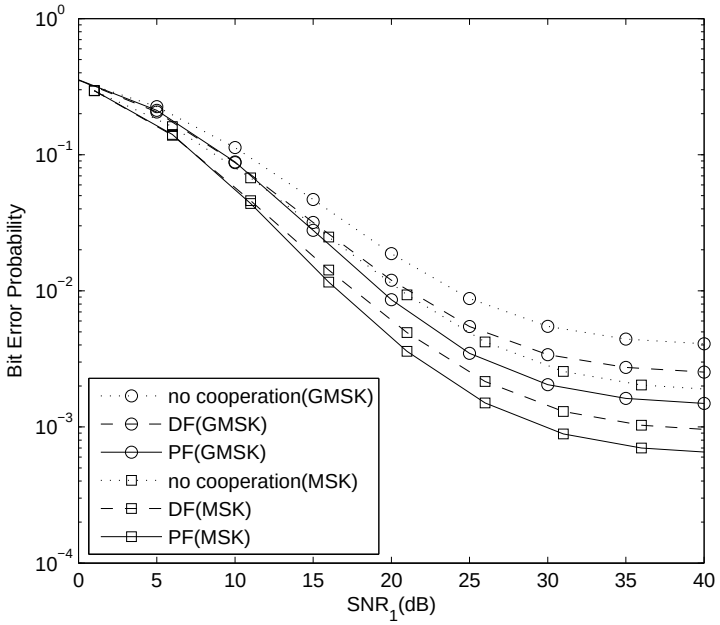

Figure 4.6: Analytical results for GMSK and MSK at $f_D T = 0.03$.

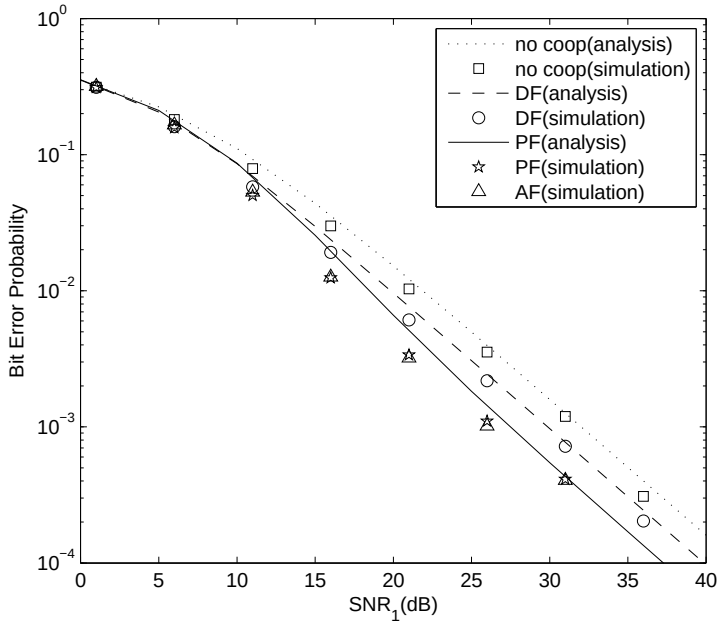

Figure 4.7: Comparison between analytical and simulation results for GMSK at $f_D T = 0$.

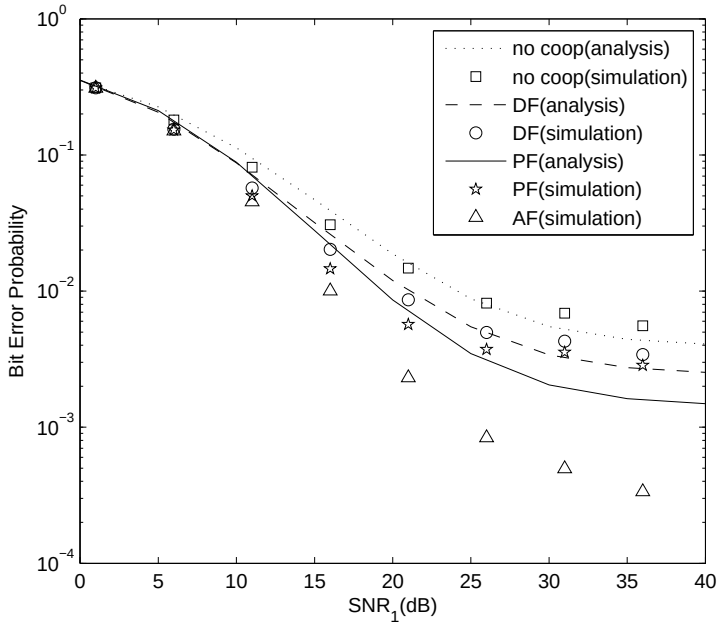

Figure 4.8: Comparison between analytical and simulation results for GMSK at $f_D T = 0.03$.

4.2 PF-CPFSK with Dual Antenna Selection

In Chapter 3 we show the performance of the proposed cooperative communication system with phase-forward, decode-and-forward and amplify-and-forward. We notice that although the performance of PF is better than DF, it is not as good as AF under fast fading. In this section we proposed a possible improvement to the proposed PF scheme, namely, using dual-antenna selection at the relay.

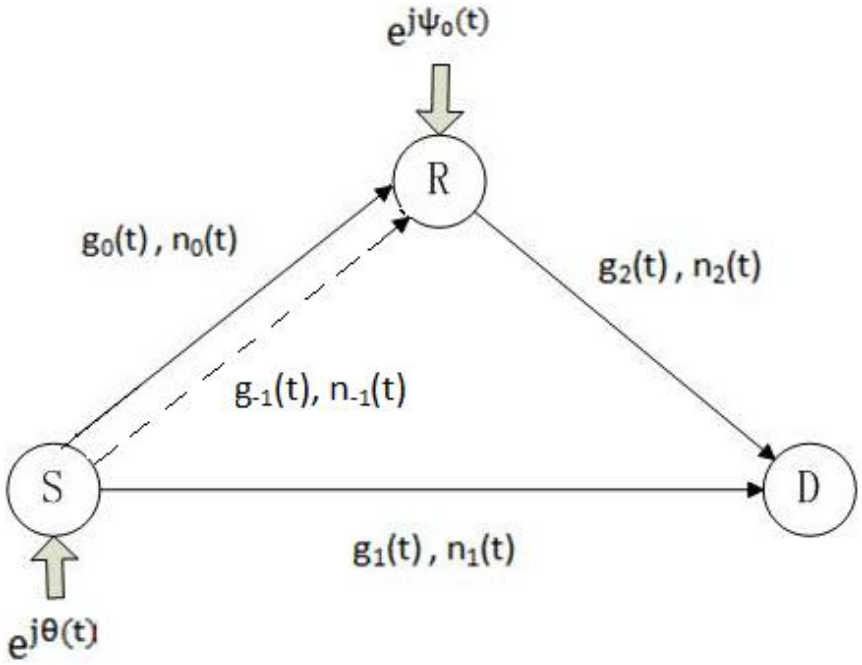

Figure 4.9: Cooperative communication model. The dash link between S and R is only relevant when there is antenna selection at the relay.

The cooperative communication system with dual-antenna selection at the relay is shown in Fig. 4.9. In this system, the relay has two copies of the original transmitted signal: the signal $r_0(t)$ in (3.4) and (3.5), as well as the signal

$$r_{-1}(t) = g_{-1}(t)\exp\{j\theta(t)\} + n_{-1}(t) = a_{-1}(t)\exp\{j\psi_{-1}(t)\}, \tag{4.10}$$

where $g_{-1}(t)$ and $n_{-1}(t)$ are the complex fading gain and noise in the second $S-R$ path, and $a_{-1}(t)$ and $\psi_{-1}(t)$ are the amplitude and phase of $r_{-1}(t)$. We assume $g_{-1}(t)$ and $n_{-1}(t)$ are statistically identical to $g_0(t)$ and $n_0(t)$ respectively. It should be pointed out that at the time the thesis was written, we only had the opportunity to consider CPFSK with dual-antenna selection. Consequently, $\theta(t)$ is that of a CPFSK signal; see (2.12).

In principle, the relay can simply forward the phase of the stronger signal to the destination. However in doing so, the phase of the forwarded signal will be discontinuous at the switching instants, a highly undesirable property from the spectral efficiency point of view. According to [30], the spectral tail of a CPM signal decays at a rate of $f^{-(2m+4)}$, where m is the number of continuous derivatives of the phase pulse. For CPFSK, its phase pulse has zero number of continuous derivatives, so its PSD decays at f^{-4}. Non-continuous phase FSK, on the other hand, has $m=-1$ continuous derivatives, so its PSD decays at f^{-2}. This means that if we can not maintain phase continuity after antenna selection at the relay, then the spectrum of the forwarded signal will follow that of discontinuous phase FSK, which is much wider than that of the original CPFSK signal. Not only will this increase the transmission bandwidth, it also means that more noise will be admitted into the destination receiver, an equally undesirable phenomenon. Fortunately, it is possible to add a phase adjustment term at each switching instant to make the forwarded phase continuous without affecting the performance of the discriminator receiver. To describe this phase adjusting technique, recall first that $a_0(t)$ and $a_1(t)$ are the amplitudes of the signals received at the relay antennas, and $\psi_0(t)$ and $\psi_1(t)$ the corresponding phases. Now let $t_0=0,t_1,t_2$ be the antenna switching instants, with $t\in[t_n,t_{n+1}]$ being the n-th switching interval and denoted by I_n. If $a_0(t)>a_{-1}(t)$ in the interval I_n, then by definition, $a_{-1}(t)>a_0(t)$ in the interval

I_{n+1}. Without loss of generality, we assume $a_0(t) > a_{-1}(t)$ in I_0, and hence the forwarded phase in this interval is $\psi_R(t) = \psi_0(t)$. The forwarded phase in subsequent intervals will alternate between $\psi_{-1}(t)$ and $\psi_0(t)$, but with proper phase adjustments. Specifically, the forwarded phase in the intervals I_{2k} and I_{2k+1}, $k = 0, 1, 2, ...$, are:

$$\psi_R(t) = \begin{cases} \psi_0(t) + \psi_R(t_{2k}) - \psi_0(t_{2k}), & t \in I_{2k}, \\ \psi_{-1}(t) + \psi_R(t_{2k+1}) - \psi_{-1}(t_{2k+1}), & t \in I_{2k+1}, \end{cases} \tag{4.11}$$

where $\psi_R(t_n) - \psi_0(t_n)$ or $\psi_R(t_n) - \psi_{-1}(t_n)$ is the phase compensation term required to maintain phase continuity. The forwarded signal itself is $\hat{s}(t) = \exp\{j\psi_R(t)\}$, with $\psi_R(0) = \psi_0(0)$ being the initial forwarded phase.

If we evaluate the first line of (4.11) at its starting time t_{2k}, then we end up with $\psi_R(t_{2k})$ on both sides of the equation. Similarly, if we substitute $t = t_{2k+1}$ into the second line of (4.11), we have $\psi_R(t_{2k+1})$ on both sides. These results simply mean that the phase adjustment scheme described in (4.11) is indeed able to maintain phase continuity at the switching instants. In addition, it is observed from (4.11) that the forwarded phase derivative depends only on the phase derivative of the signal being selected and not on the phase adjustment. This property ensures that the discriminator detector can be used to detect the data received over the selected antenna.

To gain a better understanding of (4.11), lets study how the forwarded phase evolves over time in the first three switching intervals. In the interval I_0, the forwarded phase is simply $\psi_R(t) = \psi_0(t)$, $0 \le t \le t_1$, according to the first line of (4.11). In the next interval I_1, according to the second line of (4.11), the forwarded phase is $\psi_R(t) = \psi_{-1}(t) + (\psi_R(t_1) - \psi_{-1}(t_1))$, $0 \le t \le t_1$. Since $\psi_R(t_1) = \psi_0(t_1)$ according to the phase trajectory in the previous interval I_0, we can rewrite the "current" phase segment as

$\psi_R(t) = \psi_{-1}(t) + (\psi_0(t_1) - \psi_{-1}(t_1))$, $0 \leq t \leq t_1$. How about the forwarded phase in the interval I_2? Switching back to the first line of (4.11), we have the forwarded phase trajectory $\psi_R(t) = \psi_0(t) + \psi_R(t_2) - \psi_0(t_2)$, $t_2 \leq t \leq t_3$. According to the phase trajectory in the previous interval I_1, the forwarded phase at t_2 is $\psi_R(t_2) = \psi_{-1}(t_2) + (\psi_0(t_1) - \psi_{-1}(t_1))$. This means the phase trajectory in the interval I_2 can be rewritten as $\psi_R(t) = \psi_0(t) + (\psi_0(t_1) - \psi_{-1}(t_1)) - (\psi_0(t_2) - \psi_{-1}(t_2))$, $t_2 \leq t \leq t_3$. This procedure can be repeated for subsequent intervals and eventually one comes to the conclusion that (4.11) is equivalent to:

$$\psi_R(t) = \begin{cases} \psi_0(t) + \sum_{n=1}^{2k} (-1)^{n+1} (\psi_0(t_n) - \psi_{-1}(t_n)), & t \in I_{2k}, \\ \psi_{-1}(t) + \sum_{n=1}^{2k+1} (-1)^{n+1} (\psi_0(t_n) - \psi_{-1}(t_n)), & t \in I_{2k+1}, \end{cases} \tag{4.12}$$

with

$$\Delta\psi_R(t_n) = (-1)^{n+1} (\psi_0(t_n) - \psi_{-1}(t_n)) \tag{4.13}$$

being the actual phase-adjustment term applied at time t_n. Fig. 4.10 shows sample transmitted and received phase trajectories generated from simulation and the corresponding forwarded phase after antenna selection at the relay. It is observed that the forwarded phase trajectory closely resembles the transmitted data phase and runs parallel to it. Most important of all, there are no abrupt phase jumps at the switching instants.

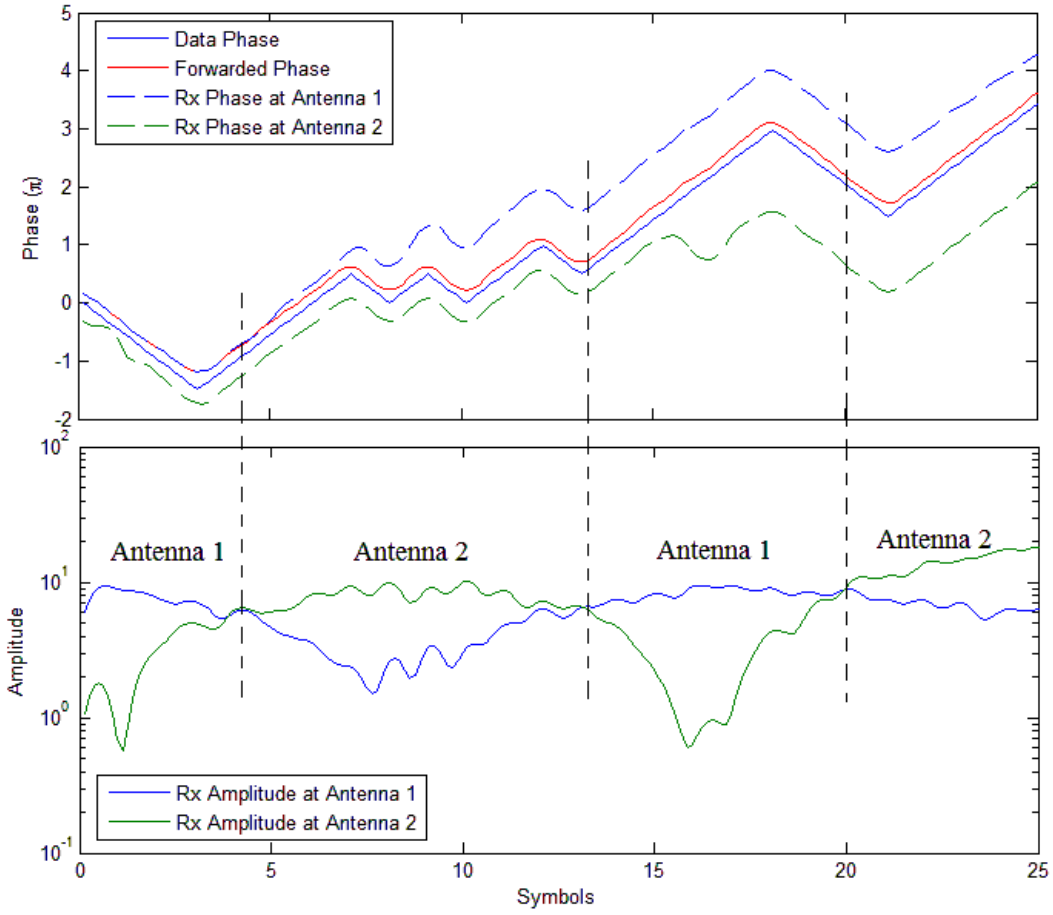

Figure 4.10: Phase adjustment scheme for dual-antenna selection: (a) sample phase diagram, and (b) corresponding amplitude diagram. The SNR in each of the two diversity paths at the relay is 24 dB and the normalized Doppler frequency is $fdT = 0.03$. All phases are normalized by π radian. The vertical bars denote switching instants.

4.2.1 BEP Analysis

We analyze next the BEP of the proposed PF-CPFSK scheme with dual antenna selection. First, we modify (3.19) to

$$P_b = \int_{-\infty}^{\infty} \Pr[D<0|\dot{\psi}_R] p(\dot{\psi}_R|\dot{\theta}=\pi h/T) d\dot{\psi}_R, \tag{4.14}$$

where $\dot{\psi}_R$ is the derivative of the forwarded phase. This phase derivative equals $\dot{\psi}_0$ when $a_0 > a_{-1}$ and equals $\dot{\psi}_{-1}$ otherwise; see (4.13). The conditional probability $\Pr[D<0|\dot{\psi}_R]$ is identical to (3.16) while the marginal pdf of $\dot{\psi}_R$ is determined as follows.

Let $F(\phi) = \Pr(\dot{\psi}_R < \phi|\dot{\theta}=\pi h/T)$ be the cumulative density function (CDF) of $\dot{\psi}_R$ under the condition that $\dot{\theta}=\pi h/T$. Clearly,

$$F(\phi) = \Pr(\dot{\psi}_0 < \phi, a_0 > a_{-1}|\dot{\theta}=\pi h/T) + \Pr(\dot{\psi}_{-1} < \phi, a_{-1} > a_0|\dot{\theta}=\pi h/T). \tag{4.15}$$

Since we assume $g_{-1}(t)$ and $n_{-1}(t)$ are statistically identical to $g_0(t)$ and $n_0(t)$, the two components in (4.15) are identical and therefore

$$\begin{aligned} F(\phi) &= 2\Pr(\dot{\psi}_0 < \phi, a_0 > a_{-1}|\dot{\theta}=\pi h/T) \\ &= 2\int_{a_0=0}^{\infty}\int_{\dot{\psi}_{0=-\infty}}^{\phi}\int_{a_{-1}=0}^{a_0} p(a_0,a_{-1},\dot{\psi}_0|\dot{\theta}=\pi h/T) da_{-1} d\dot{\psi}_0 da_0. \end{aligned} \tag{4.16}$$

This equation can be further rewritten as

$$F(\phi) = 2\int_{a_0=0}^{\infty}\int_{\dot{\psi}_{0=-\infty}}^{\phi} p(a_0,\dot{\psi}_0|\dot{\theta}=\pi h/T) \cdot \left(\int_{a_1=0}^{a_1} p(a_{-1}|\dot{\theta}=\pi h/T) da_{-1} \right) da_0 d\dot{\psi}_0, \tag{4.17}$$

because the two $S-R$ links are independent. The two conditional pdfs $p(a_0,\dot{\psi}_0|\dot{\theta}=\pi h/T)$ and $p(a_{-1}|\dot{\theta}=\pi h/T)$ in (4.17) can be obtained from (2.21) by first adding the indices 0 and -1 to various terms in that equation respectively, followed by proper marginalizations. Once these pdfs are found, they can be substituted into (4.17) to obtain an analytical expression

for $F(\phi)$. Finally, by taking the derivative of $F(\phi)$ with respect to ϕ followed by a change in notation from ϕ back to $\dot{\psi}_R$, we obtain the pdf of the derivative of the forwarded phase

$$p\left(\dot{\psi}_R|\dot{\theta}=\pi h/T\right)=\frac{\beta_0^2}{\alpha_0^2}\left(1-\rho_0^2\right)\left\{\begin{array}{l}\left[\left(\dot{\psi}_R-\rho_0\frac{\beta_0}{\alpha_0}\right)^2+\frac{\beta_0^2}{\alpha_0^2}\left(1-\rho_0^2\right)\right]^{-\frac{3}{2}}\\ -\quad\left[\left(\dot{\psi}_R-\rho_0\frac{\beta_0}{\alpha_0}\right)^2+\frac{2\beta_0^2}{\alpha_0^2}\left(1-\rho_0^2\right)\right]^{-\frac{3}{2}}\end{array}\right\}. \quad (4.18)$$

This pdf can then be substituted into (4.14) to obtain the BEP of phase-forward with dual-antenna selection at the relay.

For decode-and-forward, we can simply substitute $\Pr(\dot{\psi}_R<0|\dot{\theta}=\pi h/T)$ and $\Pr(\dot{\psi}_R>0|\dot{\theta}=\pi h/T)$ for $\Pr(\dot{\psi}_0<0|\dot{\theta}=\pi h/T)$ and $\Pr(\dot{\psi}_0>0|\dot{\theta}=\pi h/T)$ in (3.20). $\Pr(\dot{\psi}_R<0|\dot{\theta}=\pi h/T)$ and $\Pr(\dot{\psi}_R<0|\dot{\theta}=\pi h/T)$ can be obtained from integration of $p\left(\dot{\psi}_R|\dot{\theta}=\pi h/T\right)$ in (4.18).

Finally, we like to point out that the idea of phase forward and antenna selection is not confined to CFPSK. We can employ GMSK instead. However, due to time limitation, the analysis for phase-forward GMSK with dual-antenna selection is not included in this thesis.

4.2.2 Simulation Results

We present in this section analytical and simulation results for the BEP of the proposed PF non-coherent CPFSK scheme with dual-antenna selection as a function of the $S-D$ link's $\mathrm{SNR}_1=\gamma_1/\sigma_n^2$. The SNRs in the other two links in the cooperative network can be different from SNR_1 though. In any event, unless otherwise stated, the results shown are for the case of equally strong links and identical Doppler frequency in all the links.

In Fig. 4.11 we show the analytical BEP results of PF-CPFSK with dual-antenna selection with different doppler frequency. Similar to PF-CPFSK and PF-GMSK without

antenna selection, the BEP increases with the fade rate. However, even with a high Doppler of $f_D T = 0.03$, there is no noticeable irreducible error floor!

In Fig. 4.12 we compare the analytical BEP results of PF-CPFSK with dual-antenna selection with PF-CPFSK without antenna selection under static fading. As expected, PF-CPFSK with dual-antenna selection performs better than without antenna selection. Specifically, a clear second order diversity effect is observed in the former case. In contrast, without antenna selection, the BEP only decays inversely with the SNR.

Fig. 4.13 is the same as Fig. 4.12 except that we now consider "fast" fading with a Doppler frequency of $f_d T = 0.03$. Again, it is shown that PF-CPFSK with dual-antenna selection performs better than without antenna selection. Not only is there a second order diversity effect at intermediate SNRs, the irreducible error floor of PF-CPFSK with antenna selection is dramatically suppressed when compared to the case of no antenna selection.

Fig. 4.14 illustrates the impact dual-antenna selection has on the BEP of the proposed phase-only forward MSK scheme (PF-MSK). Also shown are the results of MSK with amplify-and-forward (AF-MSK) but no antenna selection, and the results with an ideal $S-R$ link, i.e. when the forwarded signal equal the signal transmitted by the source. It is evident that PF-MSK with dual-antenna selection performs substantially better than AF-MSK without antenna selection. The loss in amplitude information in phase-only forward is more than compensated by the presence of an extra antenna at the relay. This extra antenna creates a really strong link between the source and the relay and this leads to an approximated second order diversity effect in the BEP curve. Interestingly, the BEP of PF with dual-antenna selection is only slightly worse than that of an ideal $S-R$ link, hinting that little will be gained if we incorporate antenna selection into AF. Indeed, simulation

has confirmed that AF with dual antenna selection has practically the same BEP as PF with dual-antenna selection. As shown in the sample plot in Fig. 4.10, the forwarded amplitude, i.e. the higher of the two amplitude curves in the lower sub-figure, would stay relatively constant after AF and antenna selection, making the difference between AF and PF inconsequential.

Finally, we like to address the effectiveness of cooperative transmission against time diversity. For a static fading channel, there is no opportunity for time-diversity and cooperative transmission will always be more efficient than direct transmission with a repetition code. This is quite evident from the GMSK results in Figs. 4.5 and 4.7. In a time-selective fading channel though, one can drop cooperative transmission altogether and simply employs a rate 1/2 repetition code on the $S-D$ to achieve the same throughput and the same diversity order as the cooperative communication system in Fig. 4.9. Shown in Fig. 4.15, we found that it is indeed the case from the BEP standpoint. However, in the presence of large scaling fading (on top of time-selective fading) where the system's outage probability is the main concern, then once again cooperative transmission is preferred over time diversity. Fig. 4.16 shows the outage probability of the proposed PF-CPFSK scheme with dual antenna selection in a system where the SNR in the $S-D$ and $R-D$ links exhibit log-normal fading with a variance of 8 dB while the SNR in the $S-R$ link is static (i.e. no shadowing). Also shown in Fig. 4.16 are results for CPFSK with time diversity. The different curves correspond to different BEP thresholds that define outage: BEP of 10^{-2}, 10^{-3}, and 10^{-4}. At an outage probability of 10^{-3}, cooperative transmission consistently provides a 2 dB improvement in power efficiency over time diversity, irrespective of the BEP threshold.

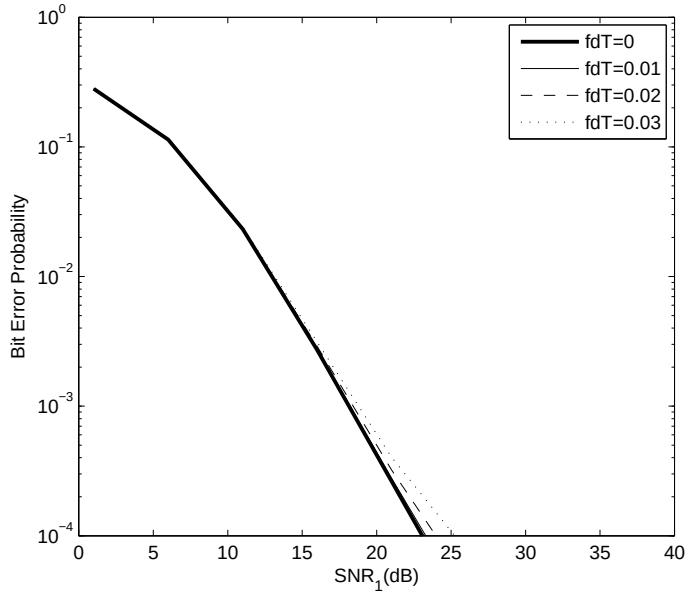

Figure 4.11: Analytical results of PF-CPFSK with dual antenna selection with different $f_D T$; equally strong links.

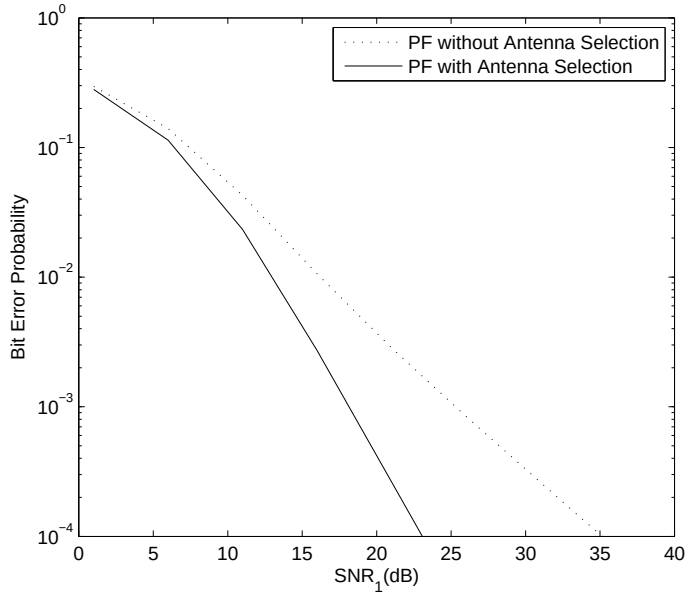

Figure 4.12: Analytical results of PF-CPFSK with & without dual antenna selection; $f_D T = 0$; equally strong links.

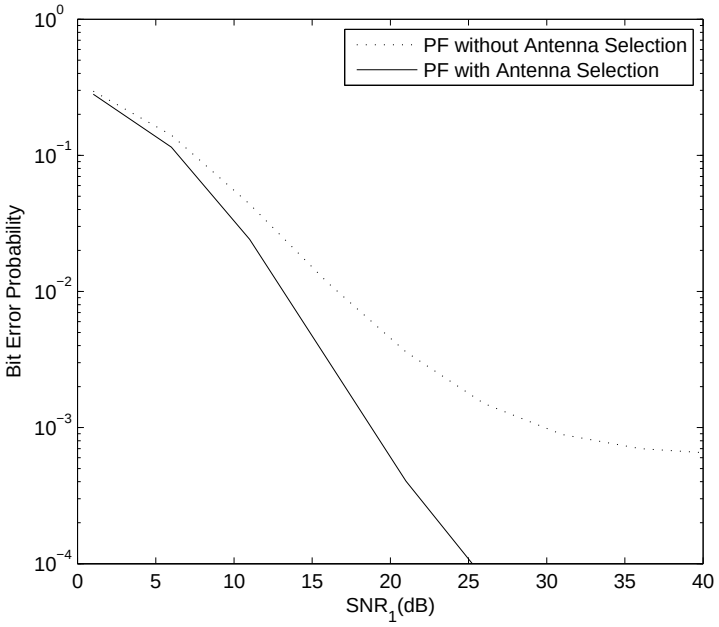

Figure 4.13: Analytical results of PF-CPFSK with & without dual antenna selection; $f_D T = 0.03$; equally strong links.

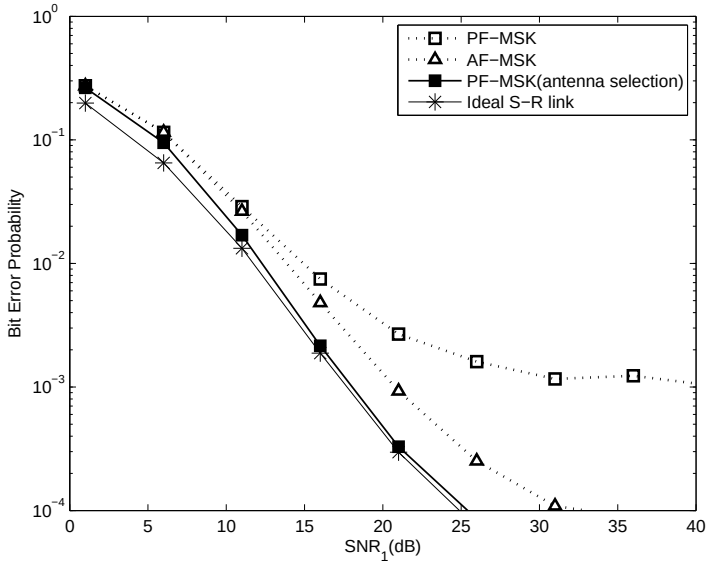

Figure 4.14: BEP of MSK with phase-only forward and dual antenna selection; $f_D T = 0.03$; equally strong links. Also shown are results with an ideal $S-R$ link.

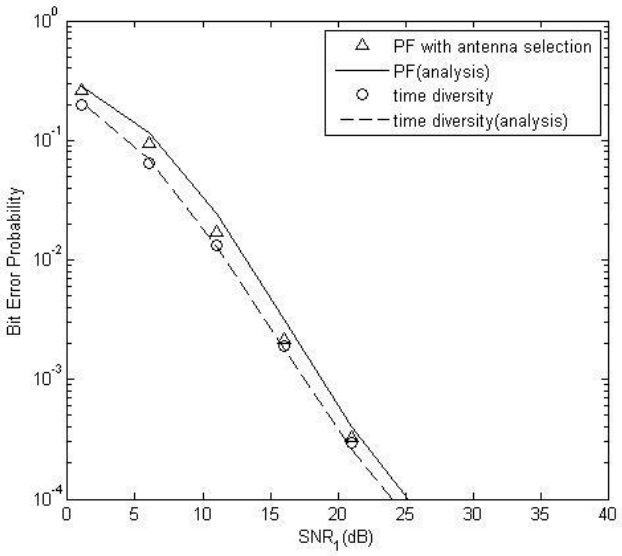

Figure 4.15: PF-CPFSK with dual-antenna selection versus time diversity from an BEP probability standpoint; $f_D T = 0.03$; equally strong links.

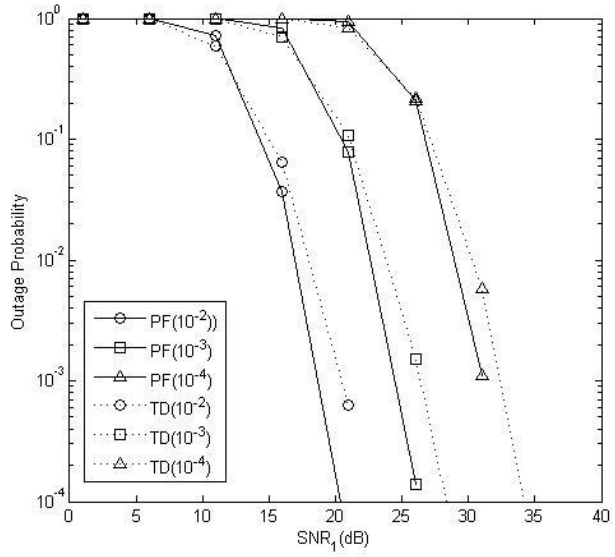

Figure 4.16: PF-CPFSK with dual-antenna selection versus time diversity from an outage probability standpoint; $f_D T = 0.03$, 8 dB lognormal fading in S-D and R-D links, no shadowing in the S-R link.

Chapter 5

Conclusion

5.1 Conclusion

Because of its constant-envelop property, continuous modulation (CPM) has found applications in cellular and private radio communication systems. Specifically, it enables these systems to use inexpensive Class C power amplifiers. We propose in the thesis the concept of Phase-only Forward as a possible relay strategy for cooperative communication involving CPM. The new technique enables the relay nodes to maintain constant envelop signaling without the need to perform decoding and signal regeneration. It is thus simpler than conventional decode-and-forward. To further reduce receiver complexity in a time-selective fading environment, we advocate the adoption of discriminator detection at the destination node. We test this PF concept with two CPM scheme known as continuous phase frequency shift keying (CPFSK) and Gaussian minimum shift keying (GMSK). Specifically, semi-analytical expressions for the BEP of phase-forward, non-coherent, CPFSK and GMSK cooperative transmission schemes are derived in the paper for cases

with and without antenna selection at the relay. In addition, for the antenna selection case, we propose a novel phase-adjustment scheme that allows the relay node to maintain phase continuity at the antenna-switching instants. Our BEP analysis is general in the sense that it allows the different links to have different Doppler frequencies and signal-to-noise ratios - a situation typical of an inter-vehicular communication system. It is found that even without antenna selection at the relay, PF has a lower BEP than conventional decode-and-forward (DF). It also delivers the same performance as amplify-and-forward (AF) when fading is static. In a time-selective fading environment, PF is not as efficient as AF when antenna selection is not available at the relay. However, if dual-antenna selection at the relay, the PF and AF have practically the same performance even with time-selective fading. The conclusion is thus reached that for constant envelop modulation, PF has lower implementation cost than both AF and DF. There is no need to use costly linear amplifier (as in the case of AF) and there is no need to do any decoding and signal regeneration at the relay (as in the case of DF). The following summarizes the major contributions of the thesis:

1. We propose the idea of PF, which has not been considered in the literature. Most importantly for constant envelop modulation, we demonstrate that it works at least as good as existing forwarding strategies but at lower implementation cost.

2. We address time-selective fading in cooperative communication, which to our best knowledge, had not been considered in the literature.

3. We were able to derive semi-analytical results for this complicated system, which is by no mean trivial.

4. We propose a phase-compensation scheme to maintain phase-continuity at the relay

when antenna selection is employed.

5.2 Suggestion for Future Work

There are some possible future extensions to this thesis. Firstly, because of time limitation, we only analyzed the performance of GMSK cooperation transmission without antenna selection in this thesis. To analyze the performance of GMSK with antenna selection, the procedure developed in Chapter 4 for CPFSK with dual antenna selection can be adopted. In addition, we can extend the current investigation to multi-level CPM.

Secondly, we should point out that the proposed idea of phase-forward is not only limited to CPM signals. As we shown in Chapter 3 for DBPSK signal, PF still offers a better performance than conventional DF. Considering the low system complexity and inexpensive non-linear amplifier advantages, the performance analysis of the proposed PF scheme with other modulation schemes besides CPM could be done in the future.

Finally, this performance analysis is based on the cooperation transmission model shown in Chapter 2, and this model adopts the so-called protocol II in [5]. There are some other protocols proposed in the literature and the performance of PF with those protocols could also be analyzed, for example, some of the 2-way relaying protocols recently proposed in the literature. Also, besides discriminator detection, we can consider other detection strategies and examine how they impact the performance.

Appendix A

Power Spectrum Density of CPM Signal

A.1 Power Power Spectrum Density of CPFSK Signal

From [14], we know the power spectrum of a CPFSK signal can be expressed as

$$\Phi_{vv}(f) = T\left[\frac{1}{M}\sum_{n=1}^{M} A_n^2(f) + \frac{2}{M^2}\sum_{n=1}^{M}\sum_{m=1}^{M} B_{nm}(f)A_n(f)A_m(f)\right], \tag{A.1}$$

where

$$A_n(f) = \frac{\sin\left(\pi\left[fT - \frac{1}{2}(2n-1-M)h\right]\right)}{\pi\left[fT - \frac{1}{2}(2n-1-M)h\right]}, \tag{A.2}$$

$$B_{nm}(f) = \frac{\cos(2\pi fT - \alpha_{nm}) - \psi\cos\alpha_{nm}}{1+\psi^2 - 2\psi\cos(2\pi fT)}, \tag{A.3}$$

$$\alpha_{nm} = \pi h(m+n-1-M), \tag{A.4}$$

$$\psi \equiv \psi(jh) = \frac{\sin M\pi h}{M\sin\pi h}. \tag{A.5}$$

h is the modulation index and M is the number of possible values of modulated data.

From these equations, we can obtain the 99% and 99.9% bandwidth of the CPFSK

signal, by computing S_{band}/S_{total}, where

$$S_{total} = \int_{-\infty}^{\infty} \Phi_{vv}(f)df, \tag{A.6}$$

and

$$S_{band} = \int_{-B/2}^{B/2} \Phi_{vv}(f)df. \tag{A.7}$$

This is how we obtain the normalized bandwidth of the binary CPFSK schemes listed in Table2.1.

A.2 Power Spectrum Density of CPM Signal

From [14] we know the power spectrum of a CPM signal is

$$\begin{aligned}\Phi_{vv}(f) = 2\Big[&\textstyle\int_0^{LT} \bar{\varphi}_{vv}(\tau)cos(2\pi f\tau) \\ &+\frac{1-\psi(jh)cos(2\pi fT)}{1+\psi^2(jh)-2\psi(jh)cos(2\pi fT)} \textstyle\int_{LT}^{(L+1)T} \bar{\varphi}_{vv}(\tau)cos(2\pi f\tau)\,d\tau \\ &-\frac{\psi(jh)sin(2\pi fT)}{1+\psi^2(jh)-2\psi(jh)cos(2\pi fT)} \textstyle\int_{LT}^{(L+1)T} \bar{\varphi}_{vv}(\tau)sin(2\pi f\tau)\,d\tau\Big],\end{aligned} \tag{A.8}$$

where

$$\bar{\varphi}_{vv}(\tau) = \frac{1}{2T}\int_0^T \prod_{k=1-L}^{[\tau/T]} \frac{1}{M}\frac{\sin 2\pi hM\left[q\left(t+\tau-kT\right)-q\left(t-kT\right)\right]}{\sin 2\pi h\left[q\left(t+\tau-kT\right)-q\left(t-kT\right)\right]}dt, \tag{A.9}$$

and

$$q(t) = \int_0^t g(\tau)d\tau. \tag{A.10}$$

Therefore, the bandwidth occupancy of CPM depends on modulation index h and the pulse shape $g(t)$. Specifically, the $g(t)$ of a CPFSK signal is a rectangular function

$$g(t) = \begin{cases} 1/T & 0 < t < T \\ 0 & otherwise \end{cases}, \tag{A.11}$$

and the pulse of a GMSK signal is

$$g(t) = \left\{ Q\left[2\pi B\left(t-\frac{T}{2}\right)\Big/(\ln 2)^{1/2}\right] - Q\left[2\pi B\left(t+\frac{T}{2}\right)\Big/(\ln 2)^{1/2}\right]\right\}. \qquad \text{(A.12)}$$

By using these equations we can obtain the corresponding bandwidth of a CPM signal. Moreover, a large modulation index h usually corresponds to a large bandwidth occupancy, as we show in Fig.2.3, 2.4 and 2.5 in the CPFSK case.

Appendix B

Maximum Likelihood Non-Coherent Detection

The decision rule of the non-coherent detector adopted in this thesis was presented earlier in (3.9) and is repeated below for convenience

$$\hat{b}_k = \arg \max_{b=-1,+1} \left\{ p(a_1, \dot{a}_1, \dot{\psi}_1 | \dot{\theta} = \pi bh/T) p(a_2, \dot{a}_2, \dot{\psi}_2 | \dot{\psi}_R = \pi bh/T) \right\}. \tag{B.1}$$

From (2.22), the product of the two conditional pdfs in the decision rule is

$$\begin{aligned} & p(a_1, \dot{a}_1, \dot{\psi}_1 | \dot{\theta} = \pi bh/T) p(a_2, \dot{a}_2, \dot{\psi}_2 | \dot{\hat{\theta}} = \pi bh/T) = \\ & \frac{a_1^2 a_2^2}{\left[2\pi\alpha^2\beta^2(1-\rho^2)\right]^2} \exp\left\{ -\frac{\dot{a}_1^2 + \dot{a}_2^2}{2\beta^2(1-\rho^2)} \right\} \\ & \times \exp\left\{ -\frac{a_1^2}{2\beta^2(1-\rho^2)} \left[\left(\dot{\psi}_1 - \rho\frac{\beta}{\alpha} \right)^2 + \frac{\beta^2}{\alpha^2}\left(1-\rho^2\right) \right] \right\} \\ & \times \exp\left\{ -\frac{a_2^2}{2\beta^2(1-\rho^2)} \left[\left(\dot{\psi}_2 - \rho\frac{\beta}{\alpha} \right)^2 + \frac{\beta^2}{\alpha^2}\left(1-\rho^2\right) \right] \right\}, \end{aligned} \tag{B.2}$$

where $\alpha^2 = \gamma + \sigma_n^2$, $\beta^2 = \gamma\dot{\theta}^2 + 2\pi^2 f_D^2 \gamma + \pi^2 B^2 \sigma_n^2/3$, $\rho = \gamma\dot{\theta}/(\alpha\beta)$, and $\dot{\theta} = \pi bh/T$ are the same for the two conditional pdfs because of the iid assumption. It is clear that the

second line of (B.2) has no impact on the decision rule and thus can be ignored. Only the exponential terms in the third and fourth line are data dependent. If we define

$$m = \rho \left| \frac{\beta}{\alpha} \right| \tag{B.3}$$

and

$$c = \frac{\beta^2}{\alpha^2} \left(1 - \rho^2\right), \tag{B.4}$$

then the natural log of the product of the last two exponential terms in (B.1) is

$$-\sum_{i=1}^{2} \frac{a_i^2}{2\beta^2(1-\rho^2)} \left[(\psi_i - bm)^2 + c \right]. \tag{B.5}$$

We want to find the $b \in \{\pm 1\}$ that minimizes this sum. It is obvious that c has no affect on the decision. So this is equivalent to minimize the metric

$$\begin{aligned} M &= \sum_{i=1}^{2} a_i^2 \left(\psi_i - bm\right)^2 \\ &= \sum_{i=1}^{2} a_i^2 \left(\psi_i^2 - 2bm\psi_i + b^2 m^2\right), \end{aligned} \tag{B.6}$$

or maximize the metric

$$M' = b \sum_{i=1}^{2} a_i^2 \psi_i. \tag{B.7}$$

The result simply means

$$\sum_{i=1}^{2} a_i^2 \psi_i \underset{b=-1}{\overset{b=+1}{\gtrless}} 0. \tag{B.8}$$

This is the optimal decision rule for the binary dual-channel limiter discriminator detector for CPFSK.

Bibliography

[1] A. Nosratinia, T. E. Hunter, and A. Hedayat, "Cooperative communication in wireless networks," *IEEE Communications Magazine*, vol. 42, no. 10, pp. 74–80, Oct. 2004.

[2] J. N. Laneman, D. N. C. Tse, and G. W. Wornell, "Cooperative diversity in wireless networks: Efficient protocols and outage behavior," *IEEE Transactions on Information Theory*, vol. 50, no. 12, pp. 3062–3080, Dec. 2004.

[3] L. Sankaranarayanan, G. Kramer, and N. B. Mandayam, "Hierarchical sensor networks: capacity bounds and cooperative strategies using the multiple-access relay channel model," in *Proceedings of First Annual IEEE Communications Society Conference on Sensor and Ad Hoc Communications and Networks*, 2004, p. 191.

[4] T. Hunter and A. Nosratinia, "Diversity through coded cooperation," *IEEE Trans. Wireless Commun.*, vol. 5, pp. 283–289, Feb. 2006.

[5] R. U. Nabar, H. Bolcskei, and F. W. Kneubuhler, "Fading relay channels: performance limits and space-time signal design," *IEEE J. Select. Areas Communications*, vol. 22, no. 6, pp. 1099–1109, Aug. 2004.

[6] J. N. Laneman and G. W. Wornell, "Distributed space-time-coded protocols for exploiting cooperative diversity in wireless networks," *IEEE Transactions on Information Theory*, vol. 49, no. 10, pp. 2415–2425, Oct. 2003.

[7] S. Yiu, R. Schober, and L. Lampe, "Distributed space-time block codingfor cooperative networks with multiple-antenna nodes," in *Proceedings of IEEE Workshop on Computational Advances in Multi-Sensor Adaptive Processing (CAMSAP)*, Puerto Vallarta, Mexico, Dec. 2005, pp. 52–55.

[8] Y. Jing and B. Hassibi, "Distributed space-time coding in wireless relay networks," *IEEE Transactions on Wireless Communication*, vol. 5, no. 12, pp. 3524–3536, Dec. 2006.

[9] P. A. Anghel and M. Kaveh, "Exact symbol error probability of a cooperative network in a rayleigh-fading environment," *IEEE Transactions on Wireless Communication*, vol. 3, no. 5, pp. 1416–1421, Sept. 2004.

[10] M. Safari and M. Uysal, "Cooperative diversity over log normal fading channels: Performance analysis and optimization," *IEEE Transactions on Wireless Communication*, vol. 7, no. 5, part 2, pp. 1963–1972, May 2008.

[11] G. Chyi, J. G. Proakis, , and C. M. Keller, "On the symbol error probability of maximum-selection diversity reception schemes over a rayleigh fading channel," *IEEE Trans. Commun.*, vol. 37, pp. 79–83, Jan. 1989.

[12] E. A. Neasmith and N. C. Beaulieu, "New results on selection diversity," *IEEE Trans. Commun.*, vol. 46, no. 5, 1998.

[13] M. Win and J. Winters, "Exact error probability expression for hybrid selection/maximal-ratio combining in rayleigh fading: A virtual branch technique," in *Proc. IEEE Globecom*, Rio de Janeiro, Brazil.

[14] J. G. Proakis, Ed., *Digital Communications*, 4th ed. New York: McGraw Hill, 2001.

[15] A. Bletsas, A. Khisti, D. Reed, and A. Lippman, "A simple cooperative diversity method based on network path selection," *IEEE J. Sel. Areas Commun.*, vol. 24, pp. 659–672, Mar. 2006.

[16] Y. Zhao, R. Adve, and T. Lim, "Improving amplify-and-forward relay networks: Optimal power allocation versus selection," in *Proc. IEEE Int. Symp. Information Theory (ISIT)*, 2006, pp. 1234–1238.

[17] A. Adinoyi and H. Yanikomeroglu, "Cooperative relaying in multiantenna fixed relay networks," *IEEE Trans. Wireless Commun.*, vol. 6, no. 2, 2007.

[18] M. Yuksel and E. Erkip, "Multiple-antenna cooperative wireless systems: A diversity multiplexing tradeoff perspective," *IEEE Trans. Inf. Theory*, vol. 53, no. 10, pp. 3371–3393, Oct. 2007.

[19] H. Mheidat and M. Uysal, "Cooperative diversity with multiple-antenna nodes in fading relay channels," *IEEE Transactions on Wireless Communication*, vol. 7, no. 8, pp. 3036–3046, Aug. 2008.

[20] S. Muhaidat, P. Ho, and M. Uysal, "Distributed differential space-time coding for broadband cooperative networks," in *accepted, IEEE VTC'09S*, Barcelona, Apr. 2009.

[21] R. Maw, P. Martin, and D. Taylor, "Cooperative relaying with cpfsk and distributed space-time trellis codes," *IEEE Communication Letters*, vol. 12, no. 5, May 2008.

[22] J. B. Anderson, T. Aulin, and C.-E. W. Sundberg, Eds., *Digital Phase Modulation*. New York: Plenum Publishing Corporation, 1986.

[23] J. W. Mark and W. Zhuang, Eds., *Wireless Communications and Networking*. Prentice-Hall, 2003.

[24] K.Kuchi and V.K.Prabhu, "Power spectral density of gmsk modulation using matrix methods," in *Proc. of IEEE MILCOM*, Atlantic City, NJ, USA, Oct. 1999.

[25] S. Elnoubi, "Analysis of gmsk with discirminator detection in mobile ratio channel," *IEEE Transactions on Vehicular Technology*, vol. VT-35.

[26] P. Merkey and E. C. Posner.

[27] D. Lee and J. Lee, "Adaptive amplify-and-forward cooperative diversity using phase feedback," in *proc., IEEE VTC'07S*, pp. 1633–1637.

[28] P. Ho and J. Kim, "On pilot symbol assisted detection of cpm schemes operating in fast fading channels," *IEEE Transactions on Communication*, pp. 337–347, Mar. 1996.

[29] Q. Yang and P. Ho, "Cooperative transmission with continuous phase frequency shift keying and phase-forward relays," in *Proc. of IEEE GLOBECOM*, Honolulu, Hawaii, USA, Nov. 2009.

[30] T. Baker, "Asymptotic behavoir of digital fm spectra," *IEEE Trans. Comm*, no. 10, pp. 1585–1589, 1974.